CHALMERS

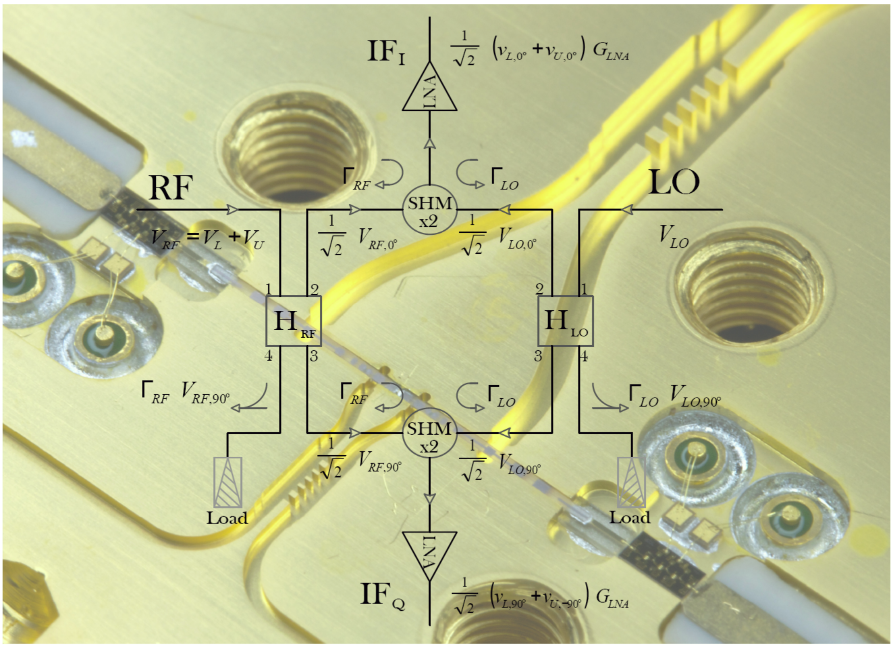

Advanced Schottky Diode Receiver Front-Ends for Terahertz Applications

PETER SOBIS

Terahertz and Millimetre Wave Laboratory
Department of Microtechnology and Nanoscience - MC2
CHALMERS UNIVERSITY OF TECHNOLOGY
Göteborg, Sweden 2011

PETER SOBIS Advanced Schottky Diode Receiver Front-Ends for Terahertz Applications 2011

Thesis for the degree of Doctor of Philosophy

Advanced Schottky Diode Receiver Front-Ends for Terahertz Applications

Peter Sobis

Terahertz and Millimetre Wave Laboratory
Department of Microtechnology and Nanoscience - MC2
Chalmers University of Technology
Göteborg, Sweden, May 2011

Advanced Schottky Diode Receiver Front-Ends for Terahertz Applications

PETER SOBIS

Doktorsavhandlingar vid Chalmers tekniska högskola
ISBN 978-91-7385-544-0
Ny serie #3225
ISSN 0346-718X

Chalmers University of Technology
Department of Microtechnology and Nanoscience - MC2
Terahertz and Millimetre Wave Laboratory
SE–412 96 Göteborg Sweden
Telephone +46 (0)31–772 1000

ISSN 1652-0769
Technical report MC2-192

Cover:
2SB Schottky diode receiver front-end assembly and circuit schematic.

Printed by Intellecta AB,
Göteborg, Sweden, 2011

Till Karin, Alisia och Alve

Abstract

This thesis treats the development of high frequency circuits for increased functionality of terahertz receiver front-ends based on room temperature Schottky diode technology. This includes the study of novel circuit integration schemes, packaging concepts as well as new measurement and characterisation techniques.

As the main result, a novel broadband waveguide integrated sideband separating (2SB) receiver topology for future Earth observation submillimetre wave instruments is proposed. The 2SB receiver topology has an inherent low RF and LO port voltage standing wave ratio (VSWR) and high sideband ratio (SBR). It is based on subharmonic (x2) Schottky diode double sideband (DSB) mixers with embedded IF low noise amplifiers (LNA's) and LO and RF 90 degree waveguide hybrids. Access to the IF IQ-paths makes it possible to implement phase and amplitude imbalance compensation schemes. Sideband separation is done in the analog domain by the use of an IF 90 degree hybrid or in the digital domain by using an IQ-correlator spectrometer. The use of embedded LNA's reduces the IF losses and leads to a low ripple and broadband response.

Measured results on a prototype 2SB receiver operating in the 320 GHz to 360 GHz frequency range show an untuned SBR of 15 dB over the whole band and mixer noise consistent with the optimal performance of a DSB mixer. The LO return loss is measured to be approximately 15 dB (broadband) and the RF return loss is estimated to have similar performance. A 340 GHz DSB receiver with an embedded custom designed 3-15 GHz LNA has also been developed. By co-simulation of the mixer and LNA using a simple mixer noise model it is shown that accurate prediction of the receiver noise response is possible. The DSB receiver exhibits ultra low noise over the 12 GHz IF bandwidth, with a minimum input receiver noise temperature of 870 K (DSB).

Two novel differential line phase shifters based on stepped impedance and coupled-line filter structures are proposed. The filters have a minimum lateral distribution making them well suited for use in submillimetre wave circuits. A method for TRL-calibration of terahertz monolithic integrated circuits (TMIC's) is also proposed and demonstrated. The method allows for embedded S-parameter characterisation of waveguide integrated TMIC devices and circuits.

Keywords: terahertz technology, terahertz electronics, submillimetre wave technology, heterodyne receivers, Schottky diodes, subharmonic mixers, sideband separating mixers, radiometers, phase shifters, differential phase shifters, S-parameter measurements, TRL-calibration, frequency converters, down converters

List of publications

Appended papers

This thesis is based on the following papers:

[A] P. Sobis, J. Stake and A. Emrich, "A Low VSWR 2SB Schottky Receiver," *submitted to IEEE Terahertz Science and Technology*, Apr. 2011.

[B] P. Sobis, N. Wadefalk, A. Emrich and J. Stake "Integration of a 340 GHz Subharmonic Schottky Diode Mixer and a LNA for Broadband and Low Noise Performance," *submitted to IEEE Terahertz Science and Technology*, Apr. 2011.

[C] P. Sobis, J. Stake and A. Emrich, "A 170 GHz 45° Hybrid for Submillimeter Wave Sideband Separating Subharmonic Mixers," *IEEE Microwave and Wireless Components Letters*, vol. 18, no. 10, pp. 680–682, Oct. 2008.

[D] P. Sobis, J. Stake and A. Emrich, "High/low-impedance transmission-line and coupledline filter networks for differential phase shifters," *IET Microwaves, Antennas and Propagation*, vol. 5, no. 4, pp. 386–392, Mar. 2011.

[E] H. Zhao, A.-Y. Tang, P. Sobis, T. Bryllert, K. Yhland, J. Stenarson and J. Stake "Submillimeter Wave S-Parameter Characterization of Integrated Membrane Circuits," *IEEE Microwave and Wireless Components Letters*, vol. 21, no. 2, pp. 110–112, Feb. 2011.

[F] P. Sobis, A. Olsen, J. Vukusic, V. Drakinskiy, S. Cherednichenko, A. Emrich and J. Stake, "Compact 340 GHz Receiver Front-Ends," *20th International Symposium on Space Terahertz Technology (ISSTT), Charlottesville, VA, USA*, pp. 183–189, Apr. 2009.

[G] P. Sobis, A. Emrich and M. Hjorth, "STEAMR Receiver Chain," *20th International Symposium on Space Terahertz Technology (ISSTT), Charlottesville, VA, USA*, pp. 320–325, Apr. 2009.

[H] A. Emrich, S. Andersson, M. Wannerbratt, P. Sobis, S. Cherednichenko, D. Runesson, T. Ekebrand, M. Krus, C. Tegnander and U. Krus, "Water Vapor Radiometer for ALMA," *20th International Symposium on Space Terahertz Technology (ISSTT), Charlottesville, VA, USA*, pp. 174–177, Apr. 2009.

Other Papers

The following papers are not included in the thesis due to an overlap in content or a content going beyond the scope of this thesis:

[a] H. Zhao, T. Ngoc Thi Do, P. Sobis, A.-Y. Tang, K. Yhland, J. Stenarsson and J. Stake, "Characterization of thin film resistors and capacitors integrated on GaAs membranes for submillimeter wave circuit applications," *23rd International Conference on Indium Phosphide and Related Materials IPRM, Berlin, Germany, 2011.*

[b] P. Sobis, J. Stake and A. Emrich, "A 340 GHz 2SB Schottky Receiver for Earth Observation Applications," *22nd International Symposium on Space Terahertz Technology (ISSTT), Tucson, AZ, USA, 2011.*

[c] A. Emrich, P. Sobis, J. Embretsen, K. Kempe, J. Jönsson and M. Krus, "STEAMR breadboard results and demonstrator status," *22nd International Symposium on Space Terahertz Technology (ISSTT), Tucson, AZ, USA, 2011.*

[d] V. Drakinskiy, P. Sobis, A.-Y. Tang, T. Bryllert and J. Stake, "Development of planar Schottky diodes," *22nd International Symposium on Space Terahertz Technology (ISSTT), Tucson, AZ, USA, 2011.*

[e] M. Wannerbratt, S. Back-Andersson, T. Ekebrand, A. Emrich, C. Emrich, J. Jönsson, M. Krus, U. Krus, D. Runesson, P. Sobis and S. Cherednichenko, "ALMA WVR final report," *22nd International Symposium on Space Terahertz Technology (ISSTT), Tucson, AZ, USA, 2011.*

[f] P. Sobis, V. Drakinskiy, J. Stake and A. Emrich, "A Low VSWR 340 GHz 2SB Schottky Receiver for Earth Observation Applications," *6th ESA Workshop on Millimetre-Wave Technology and Applications, Espoo, Finland, 2011.*

[g] V. Drakinskiy, P. Sobis, A.-Y. Tang, T. Bryllert and J. Stake, "Development of planar Schottky diodes," *6th ESA Workshop on Millimetre-Wave Technology and Applications and 4th Global Symposium on Millimeter Waves, Espoo, Finland, 2011.*

[h] J. Stake, H. Zhao, P. Sobis, A.-Y. Tang, V. Drakinskiy, A. Hülsmann, I. Kallfass, A. Tessman, A. Leuther, T. Bryllert, J. Hanning, T. Pellikka, A. Emrich, H. Richter, H.-W. Hübers, L. Yan, T. Johansen and V. Krozer "Development of a compact 557-GHz heterodyne receiver," *6th ESA Workshop on Millimetre-Wave Technology and Applications and 4th Global Symposium on Millimeter Waves, Espoo, Finland, 2011.*

[i] A. Emrich, P. Sobis, J. Embretsen and K. Kempe, "STEAMR - 340 GHz array radiometer," *6th ESA Workshop on Millimetre-Wave Technology and Applications and 4th Global Symposium on Millimeter Waves, Espoo, Finland, 2011.*

[j] M. Wannerbratt, S. Back-Andersson, T. Ekebrand, A. Emrich, C. Emrich, J. Jönsson, M. Krus, U. Krus, D. Runesson, P. Sobis and S. Cherednichenko, "ALMA WVR final report," *6th ESA Workshop on Millimetre-Wave Technology and Applications and 4th Global Symposium on Millimeter Waves, Espoo, Finland, 2011.*

[k] H. Zhao, A. Tang, P. Sobis, V. Drakinskiy, T. Bryllert and J. Stake, "Characterisation of GaAs Membrane Circuits for THz Heterodyne Receiver Applications," *21st International Symposium on Space Terahertz Technology (ISSTT), Oxford, UK, 2010.*

[l] A. Tang, P. Sobis, V. Drakinskiy, H. Zhao and J. Stake, "Parameter Extraction and Geometry Optimisation of Planar Schottky Diodes," *21st International Symposium on Space Terahertz Technology (ISSTT), Oxford, UK, 2010.*

[m] H. Zhao, A. Tang, P. Sobis, V. Drakinskiy, T. Bryllert and J. Stake, "340 GHz GaAs Monolithic Membrane Supported Schottky Diode Circuits," *GigaHertz Symposium, Lund, Sweden, 2010.*

[n] R. Dahlbäck, B. Banik, P. Sobis, A. Fhager, P. Persson and J. Stake, "A Compact 340 GHz Heterodyne Imaging System," *GigaHertz Symposium, Lund, Sweden, 2010.*

[o] P. Sobis, A. Emrich and M. Hjorth, "Receiver Chain for the STEAMR Instrument," *4th ESA Workshop on Millimetre Wave Technology and Applications, ESTEC, the Netherlands, 2009.*

[p] P. Sobis, T. Bryllert, A.Ø. Olsen, J. Vukusic, V. Drakinskiy, S. Cherednichenko, J. Stake and A. Emrich, "Development of a compact 340 GHz Receiver Front-End," *4th ESA Workshop on Millimetre Wave Technology and Applications, ESTEC, the Netherlands, 2009.*

[q] P. Sobis, J. Stake and A. Emrich, “Towards a THz Sideband Separating Subharmonic Schottky Mixer,” *19th International Symposium on Space Terahertz Technology (ISSTT), Groningen, the Netherlands, 2008.*

[r] P. Sobis, J. Stake and A. Emrich, “Towards a THz Sideband Separating Subharmonic Schottky Mixer,” *GigaHertz Symposium, Göteborg, Sweden, 2008.*

[s] P. Sobis, J. Stake and A. Emrich, “Design of a Subharmonic 340 GHz GaAs Schottky Diode Mixer on Quartz with Integrated Planar LO-IF Duplexer,” *4th ESA Workshop on Millimetre Wave Technology and Applications, Espoo, Finland, 2006.*

[t] P. Sobis, J. Stake and A. Emrich, “A simple comparison of VDI and UMS GaAs Schottky diodes for subharmonic mixers in the lower THz band,” *30th Workshop on Compound Semiconductors Devices and Integrated Circuits, WOCSDICE, Fiskebäckskil, Sweden 2006.*

[u] P. Sobis, J. Stake and A. Emrich, “Optimisation and Design of a Suspended Subharmonic 340 GHz Schottky Diode Mixer,” *IRMMW-THz Symposium, Shanghai, China, 2006.*

[v] P. Sobis, J. Stake and A. Emrich, “A 110 GHz GaAs Schottky Diode Mixer Design on Quartz with Planar LO Feed,” *GigaHertz Symposium, Uppsala, Sweden, 2005.*

[w] A. Olsen, T. Bryllert, J. Vukusic, A. Emadi, P. Sobis and J. Stake, “HBV Frequency Quintuplers,” *16th International Symposium on Space Terahertz Technology (ISSTT), Göteborg, Sweden, 2005.*

Notations and abbreviations

Notations

k_B	Boltzmann's constant
C	Capacitance
I	Current
η	Diode ideality factor
q	Elementary charge
σ	Electrical Conductivity
L	Inductance
μ	Magnetic Permeability
ε	Permittivity
h	Planck's constant
R	Resistance
T	Temperature
V	Voltage

Abbreviations

CAD	Computer Aided Design
L_M	Mixer Conversion Loss
CMB	Cosmic Microwave Background
CNC	Computerized Numerical Control
CPW	Co-Planar Waveguide
CW	Continuous Wave
DSB	Double Side Band
EM	Electro Magnetic
ESA	European Space Agency
FET	Finite Element Method
FET	Field Effect Transistor

FOM	Figure-Of-Merit
HB	Harmonic Balance
HBV	Heterostructure Barrier Varactor
IC	Integrated Circuit
IF	Intermediate Frequency
IR	Infrared
LN	Liquid Nitrogen
LNA	Low Noise Amplifier
LO	Local Oscillator
MIC	Monolithic Integrated Circuit
MMIC	Microwave Monolithic Integrated Circuit
PLL	Phase-Locked Loop
RF	Radio Frequency
RT	Room Temperature
SD	Schottky Diode
SBR	SideBand Ratio
SHIQ	SubHarmonic IQ
SHIRM	SubHarmonic Image Rejection Mixer
SHM	SubHarmonic Mixer
SSB	Single Side Band
TMIC	Terahertz Monolithic Integrated Circuit
VCO	Voltage-Controlled Oscillator
VNA	Vector Network Analyzer
VSWR	Voltage Standing Wave Ratio
WVR	Water Vapor Radiometer
2SB	Sideband Separating, Dual Sideband

Contents

Abstract **i**

List of publications **iii**

Notations and abbreviations **vii**

1 Introduction **1**
1.1 Background . . . 1
1.2 Motivation and main results . . . 3
1.3 Thesis outline . . . 7

2 Background **11**
2.1 Radiometer systems . . . 11
2.2 Receiver front-ends . . . 13
2.3 Mixer theory . . . 16
2.4 Schottky diodes . . . 18
2.5 Noise theory . . . 21

3 Mixer design **23**
3.1 Design methodology . . . 23
3.2 Circuit technology considerations . . . 23
3.3 Subharmonic (x2) mixer topologies . . . 24
3.4 E-field coupled rectangular waveguide to planar transmission line transitions . . . 25
3.5 Planar filter structures . . . 27
3.6 3D-modeling of diodes . . . 27
3.7 LO/IF filter circuit . . . 30
3.8 LO matching circuit . . . 30
3.9 RF matching circuit . . . 31
3.10 Mixer circuit design and results . . . 31
3.11 CW conversion loss measurements . . . 31
3.12 IQ Mixer design . . . 35

4 Y-factor measurements **39**

5 S-parameter characterisation of TMIC devices and circuits **45**

6 Summary of appended papers **49**

7 Conclusions and future outlook **53**

Acknowledgements **55**

Bibliography **57**

Chapter 1

Introduction

For future THz applications [1], a versatile and flexible receiver technology is needed, enabling true system integration, reducing cost and size and adding to the system functionality. This can only be done at component level and includes novel circuit integration schemes, packaging concepts as well as finding new measurement and characterisation techniques.

In this research project, advanced THz receiver topologies based on GaAs Schottky diode technology [2–5] are studied for future THz instruments and applications. Attention is given to system integration and reliability aspects as well as cost, for the possibility to transfer results directly to industrial applications. The idea is to set new standards for subsystem functionality for THz frequencies and to make it possible to define instruments focused on end user needs and requirements, instead of what is possible to implement on a component level today. In particular the main goal has been to develop a 2SB receiver topology, employing subharmonic Schottky diode mixers, for the STEAMR receiver array. The STEAMR instrument which is part of the ESA PREMIER mission [6], is specified to operate in the 320 GHz to 360 GHz frequency range with a 12 GHz wide IF bandwidth.

1.1 Background

Radio astronomy has indisputably been the main driver in the development of sensitive detectors operating in the THz range [7, 8], which is loosely defined as the electromagnetic spectrum from 100 GHz to 10 THz. Today we find advanced submillimetre wave radio telescopes like the ALMA interferometer project [9] and the APEX telescope [10], the Herschel Space Observatory [11] and COBE [12], dedicated for exploration of various aspects of the universe. The submillimetre wave band, constituting the lower part of the THz frequency band, is of great importance, as it contains a large portion of the spectral lines [13], originating from rotational and vibrational modes of basic molecules. An important part of the cosmic microwave background (CMB) radiation, originating from the very early years after Big Bang, is also found in this frequency range. Furthermore, the potential of THz-technology for new applications in the fields of medicine [14, 15], security [16], etc., is being explored. So far, the main obstacles of THz systems have been the high production costs, bulkiness, complex operation, low reliability, high maintenance e.g of cryo-coolers, and therefore, the way towards consumer applications seems still long. A promising candidate for potential "mass market" commercial THz applications is silicon technology [17].

At present, ultimate low noise heterodyne receivers used for submillimetre wave radio astronomy are based on cryogenic devices such as Superconductor-Insulator-Superconductor (SIS) tunnel junctions [18] operating up to about 1 THz reaching quantum noise levels and Hot Electron Bolometers (HEB's) [19] operating from 1 THz to about 7 THz. The development of these innovative devices has been possible thanks to advancements in processing techniques for micro and nano-scale electronics, the increase in available computational power and through the development of sophisticated CAD software. Thereto, the advancement of THz source technology and development of compact broadband source modules, using solid state amplifiers [20] and diode multipliers [21], has greatly improved the useability of heterodyne radio receivers [22] .

Another important application of submillimetre wave radiometry is remote sensing of the earth's atmosphere for which both room temperature and cryogenic technology is used. Atmospheric sensing, i.e. spectroscopy and imaging is important for the understanding of the chemical exchange mechanisms and their effects on our climate, and for accurate weather forecasting. Parameters such as temperature, pressure, wind speed and gas concentration can be extracted by studying the shape and strength of the spectral lines. Atmospheric sensing of the Earth is possible through ground based observations [23], air-born high altitude observations from aeroplanes [24,25], balloons [26] and sounding rockets [27], and by the use of space-born limb sounders and imagers like ODIN [28] and EOS MLS [29]. In contrast to radio astronomical observations, Earth observations are typically characterized by high brightness temperatures and short integration times [30].

In the study of the chemical processes that control our climate, resolving the vertical distribution of key trace gases is important, as it gives insights to the chemical interaction between the different atmospheric layers. Earth observations are also ideally made continuously (by the hour, or on daily or weekly basis) during many years, to accommodate for changes in between winter and summer as well as for naturally occurring irregularities in the climate cycle. By long term observations it is possible to detect trends and make future predictions of the climate development [6]. By the use of space born limb sounders employing tomographic scanning of the Earth's limb, continuous monitoring over many years covering large parts of the atmosphere is possible.

In Fig. 1.1 the vertical distribution of the 14 beams of the STEAMR limb sounder employing a stare-viewing concept is shown. The receiver array improves the instrument sensitivity with the square root of 14, i.e. 3.74. A high vertical resolution is possible by the use of two polarisations with overlapping beams. The altitude coverage ranges from the upper troposphere (6 km) to the lower stratosphere (28 km) denoted as the UTLS-range.

A close relationship exists between the choice of observation platform, the instrument topology and choice of receiver technology. For spaceborn atmospheric sounders, uncooled GaAs Schottky diode receivers have proven to be a feasible alternative. Being the predecessor of modern cryogenic technology, GaAs Schottky diodes have a long track record, and are based on a mature technology platform and can be produced with high reliability.

Uncooled technology has the advantage of low complexity of test equipment and facilities as well as test procedures, compared to cryogenic receiver development. Also the choice of materials, assembly procedures and more important the instrument design are simplified considerably, why Schottky technology in general is considered as an alternative with lower associated risks. In Fig. 1.2 a summary of reported receiver noise is shown, comparing Schottky diode technology with other receiver technologies.

Schottky based receiver systems can also be made very compact (low weight) and have no fundamental limitations in their operation lifetime, i.e. not limited by the amount of cooling agent that can be brought on board the satellite, which cryogenic systems typically are [12, 60]. Even though active closed cycle cooling systems like for SPICA [61] are being developed, increasing the operational lifetime and reducing the size and weight of cryogenic systems to some extent, such systems will always be subject to the limited lifetime of cryo pumps, higher complexity, and reliability concerns.

1.2 Motivation and main results

At submillimetre wave frequencies sideband separating fundamental SIS mixers have been employed for example in ALMA [9], where dual sideband (2SB) receivers are used for many of the bands reaching image rejections better then 10 dB. In this case the image band noise is rejected improving the sensitivity of the instrument by almost a factor of two. Until recently, there has been no or very little development of submillimetre wave 2SB Schottky receivers, neither for fundamental nor for subharmonic mixers. Instead, traditional filtering techniques using bulky optical or waveguide filters have been used, increasing the size, loss and cost, and thus, decreasing the performance and scientific impact of the instruments. However with the development of the STEAMR instrument, the need for 2SB functionality for Schottky receivers has been addressed. With an instrument baseline of 14 heterodyne receivers in a focal plane array, based on both DSB and 2SB subharmonic Schottky diode mixers [62] operating in the 320 GHz to 360 GHz range, the development of a robust 2SB receiver architecture has been undertaken.

For Schottky based receivers, suppression of the image band noise will not have the same impact on the system noise as for cryogenic receivers, since the receiver noise is many times larger than the antenna noise (background noise). Instead the main motivation for using SSB receivers for atmospheric observations comes from the complex spectral composition, e.g. line broadening effects and the combination of weak and strong spectral lines, see Fig. 1.3. When down-converted to the IF band signals from the upper sideband (USB) and lower sideband (LSB) interfere with each other. This can also lead to a confusion in the origin of signals. To be able to resolve the individual lines a sideband separating topology becomes desirable.

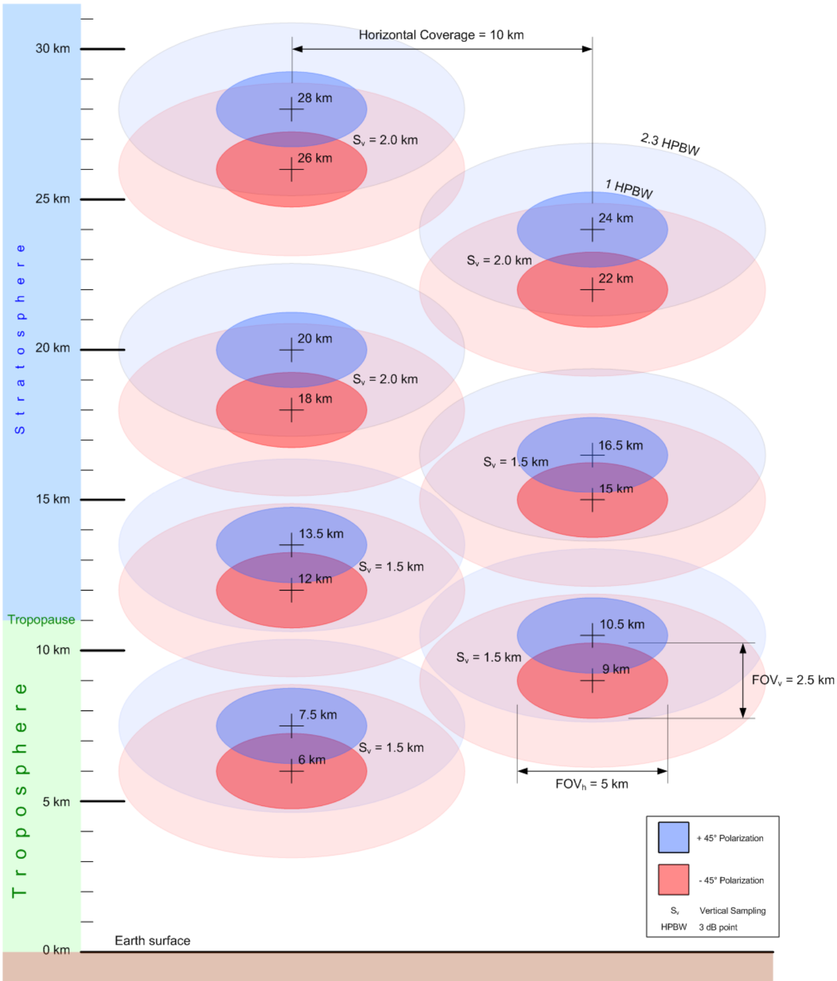

Fig. 1.1: Beam distribution of the STEAMR 14 pixel limb sounder using a stare viewing concept in 2 polarizations covering altitudes from 6 km to 28 km - courtesy of M. Ahlberg, Swedish Space Corporation (SSC).

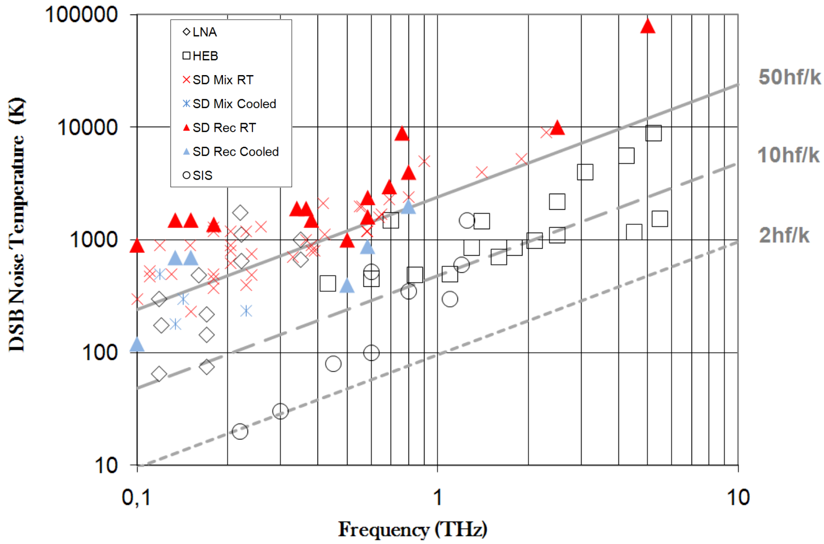

Fig. 1.2: Comparison of equivalent input DSB noise temperature results for various receiver technologies; cooled and room temperature Schottky diode mixers and receivers [19, 22, 31–52], HEB receivers [19, 53], SIS receivers [19] and various LNA's [54–59].

Moreover to be able to detect as many different molecular lines as possible and the several GHz wide lines due to pressure broadening, broad instantaneous frequency coverage is needed. For STEAMR the IF bandwidth is specified to 12 GHz for both DSB and 2SB receivers. In Table 1.1 a summary of the main targets is shown.

The most cost efficient approach for instruments that use only one or a few DSB receivers is a low level integration modular assembly i.e. individual waveguide packaged mixers, multipliers and coaxial packaged LNA's. The integration and/or custom design of front-end components is motivated, as new and higher standards are set for radiometric instruments, e.g. for receiver arrays. Integration will in general make it possible to design instruments with larger frequency coverage and allow for co-optimization and integration of components and sharing of mechanical and electrical resources. Naturally, trade offs are made when choosing integration level. Variability of components and yield are two limiting factors to consider, development cost another. In Fig. 1.4 and Fig. 1.5 the engineering models of the STEAMR instrument and receiver cartridge are shown respectively. The instrument is designed for high reliability and high sensitivity and therefor uses a multibeam system with no moving parts i.e. does not use the traditional scanning of one beam. The

Table 1.1: Main UT/LS target species in the STEAMR Band A5 instrument baseline configuration from 2010, courtesy of J. Urban, Chalmers University of Technology.

f_{lsb} = 324.0-336.0 GHz, f_{usb} = 343.25-355.25 GHz. f_{lo} = 339.625 GHz, f_{if} = 3.625-15.625 GHz.	
species	target lines
H_2O	325.152 GHz
HDO	335.395 GHz
CO	345.795 GHz
HCN	354.505 GHz
O_3	e.g. 326.900, 327.844, 332.704, 332.881, 335.271, 349.743, 352.323, 352.592, 352.815, 355.018 GHz
N_2O	326.556, 351.667 GHz
HNO_3	~ 331.9, 332.3, ~344.5 GHz
CH_3CN	~ 331.0, ~349.4 GHz
CH_3Cl	~ 345.4 GHz
(ClO)	~346.92, 352.88 GHz

total instantaneous bandwidth is nearly 200 GHz and the instrument is thus close to submillimeter wave operation in terms of processed IF bandwidth, not only operating RF frequency.

Based on previous radiometer development at submillimetre frequencies at Omnisys Instruments AB, a 2SB topology for subharmonic mixers was proposed to the Swedish Research Council (VR) in 2005 for this research project. The proposed topology consisted of a 45-degree LO phase shifter hybrid and a matched Y-junction for the RF feed, compare to the work on subharmonic IQ-mixers [63] [64] and the development of a novel sideband separating SIS mixer [65]. The main outline for realisation of the proposed 2SB receiver concept was presented in paper [C]. In papers [F,G] the first results for this topology were demonstrated together with results on a new improved 2SB Schottky receiver topology. The new topology used quadrature feeding for both the LO and RF and both demonstrators were evaluated using a modular waveguide assembly, i.e. individual mixers and hybrid blocks.

Both topologies had a nominal sideband ratio SBR of around 5-10 dB, that could be improved to around 15-20 dB by phase tuning of the IQ-imbalance. In addition, initiated as a collaboration project with Rutherford Appleton Laboratories, a parallel development and demonstration of a waveguide integrated subharmonic sideband separating mixer, based on the topology in paper [C], was also conducted [66]. The outcome of these experiments was that the improved 2SB receiver topology was choosen for further investigation.

In paper [A] the first demonstration of a waveguide integrated 2SB re-

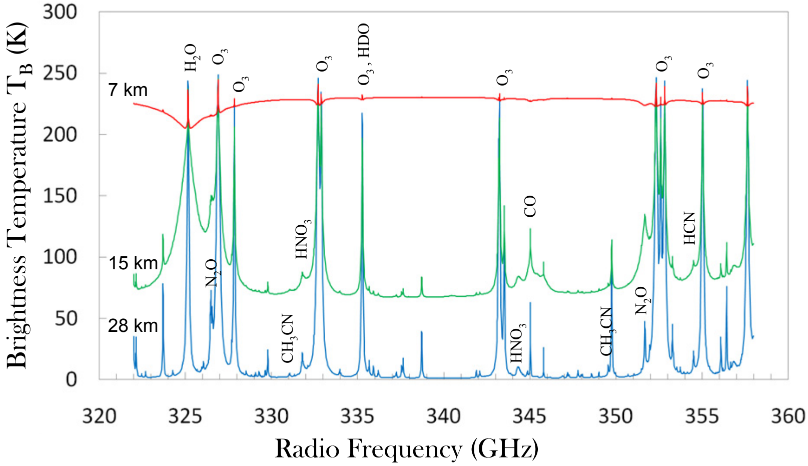

Fig. 1.3: Simulated frequency spectrum of the atmosphere at 7 km,15 km and 28 km altitude in the STEAMR frequency range - courtesy of J. Urban, Chalmers University of Technology.

ceiver topology based on quadrature feeding of both LO and RF is made with very promising results, showing a nominal sideband ratio SBR of 15 dB, and mixer noise performance close to state-of-the-art DSB mixers. Taking the results from paper [B] on a subharmonic DSB mixer with embedded custom designed LNA, the realisation of broadband high performance 2SB receivers seems feasible.

1.3 Thesis outline

This thesis treats the development of high functionality submillimetre wave receivers based on room temperature Schottky diode technology. In chapter 1, an introduction, background and motivation for this work is given. In chapter 2, a brief introduction to radiometer systems is given followed by the theory and principal operation of Schottky diode mixers. The main characteristics of modern planar GaAs Schottky diodes are discussed. In Chapter 3 the designs of the DSB mixer and IQ-mixer are discussed. In Chapter 4 the Y-factor measurement method is described and experimental results are shown. In Chapter 5 the membrane TRL calibration technique is presented. In Chapter 6 a summary of the appended papers is given and in Chapter 7 conclusions are made and the future outlook for advanced Schottky receivers

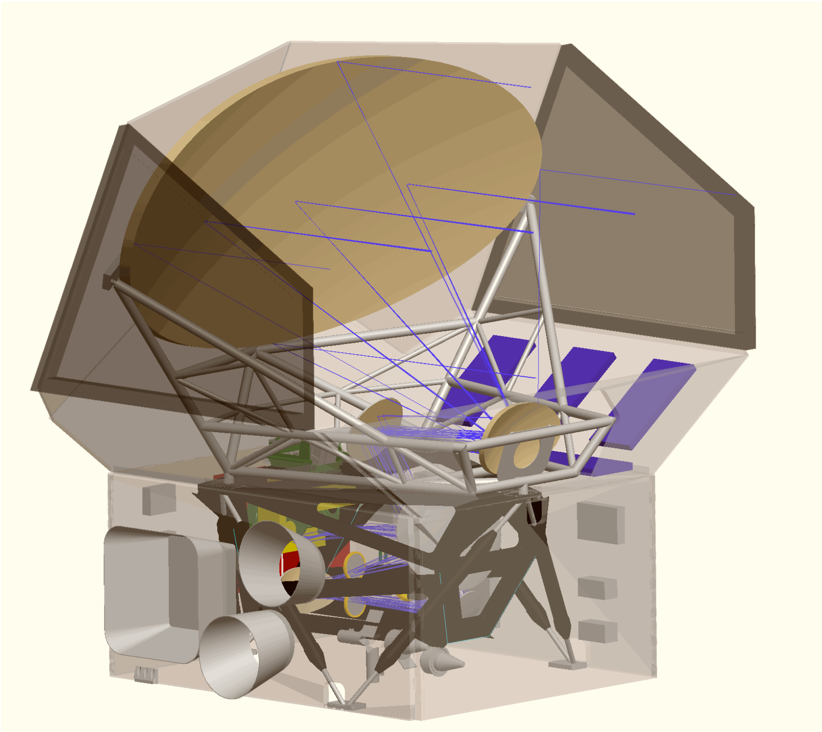

Fig. 1.4: Engineering model of the proposed STEAMR intrument showing the sun shield, the main reflector, the quasi-optical system and contours of various subsystems, e.g. spectrometers, calibration loads etc., courtesy of the Swedish Space Corporation (SSC).

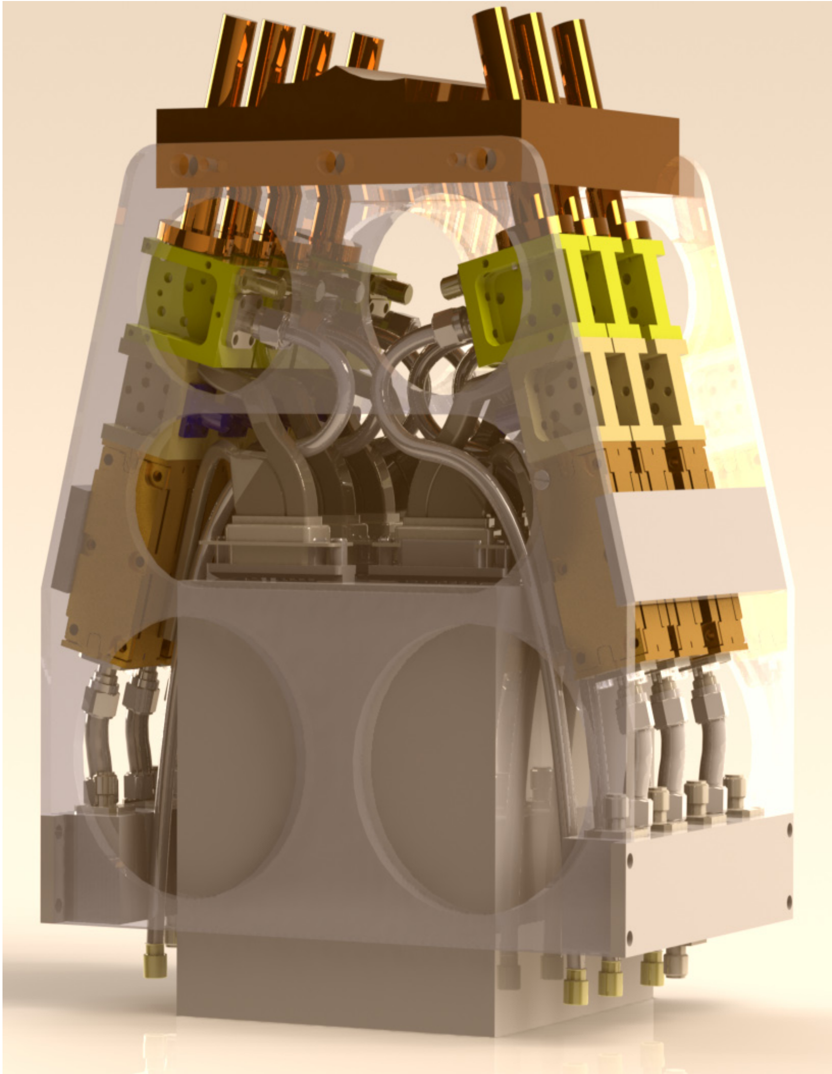

Fig. 1.5: Engineering model of the receiver cartridge developed at Omnisys Instruments AB for the STEAMR instrument, showing seven front-end receivers, each consisting of a horn antenna, a subharmonic mixer with embedded LNA, a LO varactor doubler, and an active W-band multiplier module. In the instrument, two cartridges will be used, one for each polarisation, together forming the 14 pixel stare-viewing array.

is discussed.

In the appended paper section the main results of this work are found. In paper [A], the design and characterisation of the novel waveguide integrated sideband separating (2SB) receiver, operating in the 320-360 GHz band, based on subharmonic (x2) Schottky diode mixers and embedded LNA's is presented. The advantage of co-optimization and integration of the mixer and LNA is demonstrated in paper [B]. An alternative 2SB receiver topology is proposed in paper [C], in which a possible realisation of a waveguide based 45 degree hybrid is demonstrated. As a side result two novel differential phase shifter topologies are proposed applicable for planar submillimetre wave hybrid circuits, providing an alternative to traditional waveguide based and planar differential phase shifter hybrids, see paper [D]. In paper [E] a novel approach for S-parameter characterisation of submillimetre wave membrane devices and circuits is presented. papers [F] and [G] mainly discuss different 2SB receiver implementations and the low VSWR waveguide integrated 2SB receiver topology is proposed. A subharmonic mixer design with an embedded commercial LNA is presented together with the demonstration of a broadband IF spectrometer back-end based on IQ-correlators. Also different options for the LO-source module are evaluated. Finally, in paper [H] a short summary of the ALMA Water Vapor Radiometer (WVR) development is presented.

Chapter 2

Background

This chapter describes the main theory and background information.

2.1 Radiometer systems

A radiometer can detect and measure the power of radio waves (electromagnetic radiation) in a certain frequency band. Planck's radiation law gives us the power spectral density P_{sf} emitted by a blackbody at physical temperature T at frequency f and for single mode propagation its given by:

$$P_{sf} = \frac{hf}{e^{\frac{hf}{k_B T}} - 1} \tag{2.1}$$

with k_B and h being the Boltzmann and Planck constants respectively.

By using Rayleigh-Jeans low frequency approximation of Planck's radiation law, we get a linear relationship between the antenna temperature T_A and received power P_A:

$$P_A = k_B T_A B \tag{2.2}$$

For atmospheric observations, the antenna radiometric temperature will correspond to the brightness temperature of the atmosphere. The typical brightness temperature is around 200 K at low altitudes decreasing with higher altitudes down to around 3 K (cold sky), see Fig. 1.3. The spectral emission lines of gases are seen as peaks with an increased brightness temperature at certain frequencies. The receiver is responsible for detection and quantification of this radiation which is translated to a measured value of arbitrary unit e.g. a DC voltage. The measured power will be a function of the antenna temperature T_A and radiometer temperature T_R:

$$P_{meas} = k_B B (T_A + T_R) G \tag{2.3}$$

with B being the IF predetection channel bandwidth and G being the system gain.

The sensitivity of a radiometer system corresponding to the root mean square fluctuations of the measured radiation temperature, is a function of the total noise temperature of the radiometer system $T_A + T_R$, the post detection integration time τ and predetection channel bandwidth B. For an ideal detector, i.e. the receiver noise and system gain are assumed time invariant, the sensitivity ΔT is given by the basic radiometer equation [30]:

$$\Delta T = \frac{T_A + T_R}{\sqrt{B \cdot \tau}} \tag{2.4}$$

If we keep the bandwidth fixed, which is typically determined by the specific application, then a better sensitivity can be either achieved by reducing the receiver noise or increasing the integration time. By using a multibeam system instead of traditional scanning of a single beam the integration time will also be increased e.g. a system of 16 beams with an antenna temperature of 200 K and receiver noise of 1000 K has an equivalent performance to a single beam system with a receiver noise of 100 K. The receiver noise temperatures will depend on the choice of technology and design of the receiver. The integration time will typically depend on system requirements, e.g. spatial resolution, and will be limited by system drift. Taking gain instabilities into account the radiometer equation can be written as:

$$\Delta T_{gain} = \sqrt{\frac{{T_{SYS}}^2}{B \cdot \tau} + \left(\frac{\Delta G}{G}\right)^2 {T_{SYS}}^2} \tag{2.5}$$

with ΔG being the rms fluctuations of the system gain representing an effective system gain instability.

System components will always be under the influence of varying operation conditions, e.g. ambient temperature, component oscillations, aging effects, random fluctuations etc. Therefore calibration techniques have to be applied to applications requiring a high absolute accuracy. A measure of system stability is the so called Allan variance (AVAR) [67], that was initially developed for measuring the noise and stability of clock systems. The AVAR is calculated for a finite set of N number of consecutive measurements of a certain quantity e.g. a DC voltage coming from a detector. The AVAR is defined as the variance of the difference of two consecutively measured averages ϕ. Each average is calculated on a subgroup of consecutive measurements spanning over a time τ. Each value of τ will divide the total number of measurements into M number of groups. The AVAR can be written as [68]:

$$\sigma^2_{AVAR}(\tau) = \frac{1}{2M} \sum_i (\phi(\tau)_{i+1} - \phi(\tau)_i)^2 \tag{2.6}$$

The AVAR is typically plotted in a log/log scale (Allan-plot) in which an upper limitation of the integration time can be found above which the sensitivity of the system is not improved anymore.

Stability of subsystems, e.g. bias supplies, amplifiers, detectors and LO chains can to a large degree be improved by proper mechanical and thermal design, active regulation of components and by optimising each subsystem for highest possible stability, e.g. by operating LO multipliers and driving amplifiers close to or in the saturated region rather then in the linear region and by using constant current supplies for the LNA's. The dynamic range and linearity are other important merits of the radiometer that have to be considered.

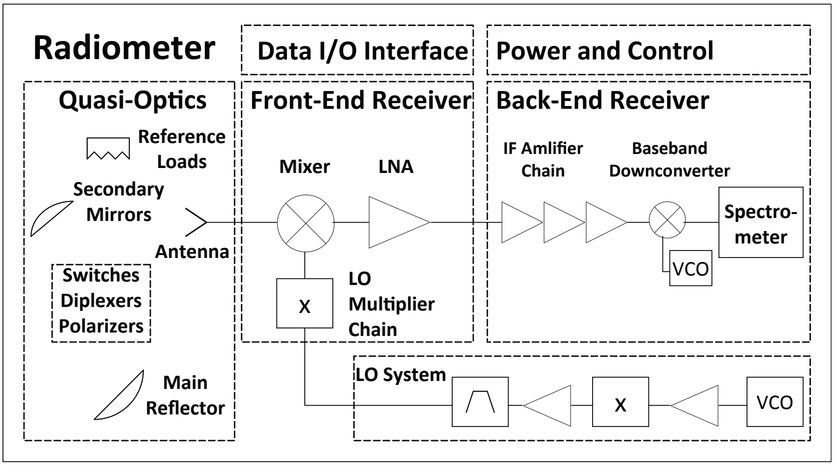

Fig. 2.1: Schematic of a Schottky based heterodyne radiometer system.

There are many different types of radiometers [30], e.g. the total power, Dicke, noise injection and correlation radiometer. The choice of receiver technology and design will differ depending on the application. For atmospheric spectrosopy the Dicke switch type calibration, which uses a reference load at the radiometer input for calibration of the received power at the antenna, is commonly used. For space-born applications cold space or thermally stabilised loads onboard the satellite could for instance be used as reference. A schematic of a general Dicke switch radiometer system based on a heterodyne receiver is sketched in Fig. 2.1. Since a considerable part of the observation is spent on calibration, this will lead to a reduced sensitivity for the ideal direct detector case (2.4). Taking gain drift instabilities into account (2.5) the system accuracy is increased manifold times.

For resolving characteristics of narrow molecular lines, a spectral resolution in the order of MHz is needed. In such applications heterodyne detectors with high resolution back-end spectrometers are typically used since RF filters with such high Q-factors become impractical. In other cases, e.g. for imaging or detection of broad features of spectral lines, spectral resolution in the order of GHz is required.

2.2 Receiver front-ends

When it comes to Schottky receiver technology, whenever the sensitivity is good enough for the specific application, the relative simple realisation and low cost of Schottky based receivers make them a natural choice. In Fig. 2.2 the layout of the 340 GHz DSB front-end receiver prototype for STEAMR, with medium integration level is shown.

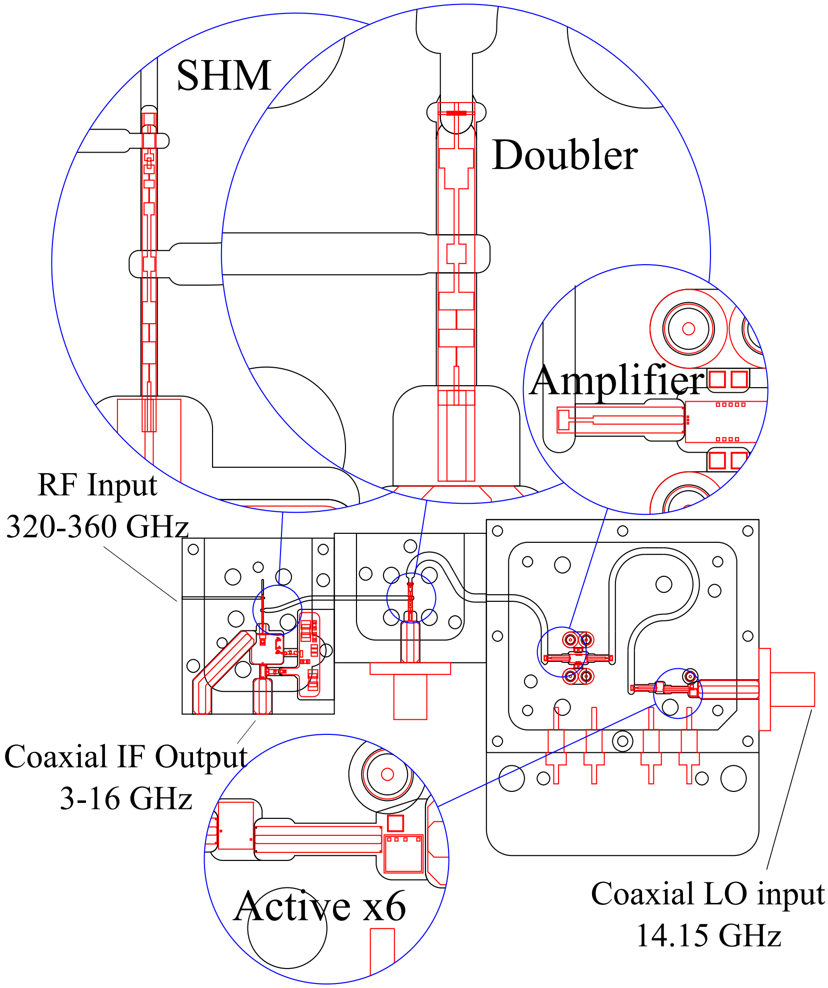

Fig. 2.2: Schematic of the STEAMR DSB front-end receiver prototype showing outline of the mechanics (black) and circuits (red) of the subharmonic mixer (SHM) with embedded LNA presented in paper [B], a varactor doubler [69] and the x6 active multiplier paper [H]. The total length of the three combined modules is 91 mm. The development has been done by Omnisys Instruments AB in collaboration with Chalmers University of Technology and Low Noise Factory.

A summary of reported state-of-the-art equivalent input noise for different THz receiver technologies is shown in Fig. 1.2 together with the lines representing 2, 10 and 50 times the quantum noise (SSB) limit. The quantum noise limit, which is a consequence of Heisenberg uncertainty principle and related to the discrete nature of energy or energy quanta discovered by Max Planck, gives a lower limit of the output noise for mixer's and LNA's [70]:

$$T_{quanta} = \frac{hf}{2k_B} \tag{2.7}$$

with f being the frequency.

Without going into the details of the noise mechanisms for the respective technologies, which is outside the scope of this thesis, we simply state that the performance of SIS technology is clearly distinguished from the other technologies approximately following the 2 x quantum noise limit (similar to LNA's at microwave frequencies) with an increasing tail up to around 1 THz at which the performance of HEB technology becomes competitive following approximately the 10 x quantum noise limit. Room temperature Schottky diode technology follows approximately the 50 x quantum noise limit. The noise performance of HEB receivers in the 1 to 10 THz range is similar to the performance of Schottky receivers in the 0.1 to 1 THz range. An interesting trend is the entrance of transistor based technology into the THz regime, competing in many aspects with both SIS and Schottky diode technologies.

Some characteristic features of state-of-the-art THz Schottky diode based receivers are:

- large IF bandwidth (often limited by LNA)
- LO power $\sim$ mW
- Receiver noise (DSB) $\sim$ 1000 K at 300 GHz to 10000 K at 3 THz
- Waveguide packaged using horn antennas

The level of LO power that is required for efficient pumping of the mixer diodes can be reduced by proper circuit design, by applying a DC bias to the diode or by using other material systems [71, 72] leading to lower turn on voltage. For Schottky diode based receivers in particular, subharmonic mixers [62], are extensively used requiring only half the LO pumping frequency with similar performance to fundamental mixers [73, 74]. The total amount of power required for generating the LO signal at half the RF frequency is considerably lower compared to receivers based on fundamental mixers. The low efficiency of multipliers and self heating effects at high power levels are the main reasons for this. Reducing the number of components and gain in the LO chain, the stability and reliability of the system will be increased.

In general for the design of efficient multiplier chains, it is necessary to optimise each multiplier stage for the specific power level and frequency range at which it will operate. For narrowband applications multiplier chains with higher efficiency can typically be designed. Another important thing to consider is of course the availability of high power amplifiers for driving the first stage of the multiplier chain. Commercially available GaN and InP HEMT based W-band (75 GHz - 110 GHz) amplifiers with output power levels from 100 mW to 0.5 W are becoming available. Various Schottky based doublers and triplers up to a couple of THz have been reported, [21]. Output powers of around 1 mW close to 1 THz, sufficient to pump a Schottky mixer, have been demonstrated using power combining techniques. Another interesting alternative suitable for high frequency high power odd harmonic generation, is the Heterostructure Barrier Varactor HBV diode [75] with an inherent symmetrical CV characteristic. The HBV does not require bias, which simplifies the circuit realisation. Moreover a similar broadband performance for HBV multipliers as for Schottky diode varactor multipliers can be achieved. At present the state of the art high frequency HBV tripler, developed at Chalmers University of Technology, is capable of generating 30 mW at 282 GHz output frequency at an input pump power of 0.5 W.

For a heterodyne Schottky receiver, the performance of the mixer and IF LNA will be equally important for the receiver noise. Thereto the phase noise and stability of the LO has to be considered. The LO amplitude stability is translated to AM noise and the phase noise have an impact on the instrument resolution. Applying Friis formula [76] the receiver equivalent input SSB noise temperature can be written as (the LO noise contribution is not included):

$$T_R = T_M + L_M \cdot T_{LNA} \tag{2.8}$$

with L_M being the mixer conversion loss, T_M the mixer equivalent input noise and T_{LNA} the LNA equivalent input noise. Thus, designing the mixer for low noise is equally important as reducing the mixer conversion loss and the LNA equivalent input noise temperature. Moreover, the RF and IF losses have to be kept at a minimum. The circuit RF losses can be reduced to some extent by partly realising the circuit in waveguide technology which has lower loss than planar implementations. The RF waveguide paths should be kept short and RF interconnects avoided if possible. Another characteristic of Schottky mixers is the high IF impedance, which is typically in the range of 150 Ω to 250 Ω. The IF mismatch between the mixer and LNA leads to a ripple response, which limits the radiometer performance. Especially for applications which require large IF bandwidths, this can become a problem, why co-design of the LNA and mixer has to be considered.

2.3 Mixer theory

A mixer converts the signal power from one frequency band to another preserving the signal phase and amplitude information through a intermodulation process with a LO signal. For a super-heterodyne downconverting mixer a very high frequency RF input signal is downconverted to a in relation low intermediate frequency IF signal, see Fig. 2.3. The mixer efficiency is measured as the ratio of the input signal power to the output signal power defined as the mixer conversion loss:

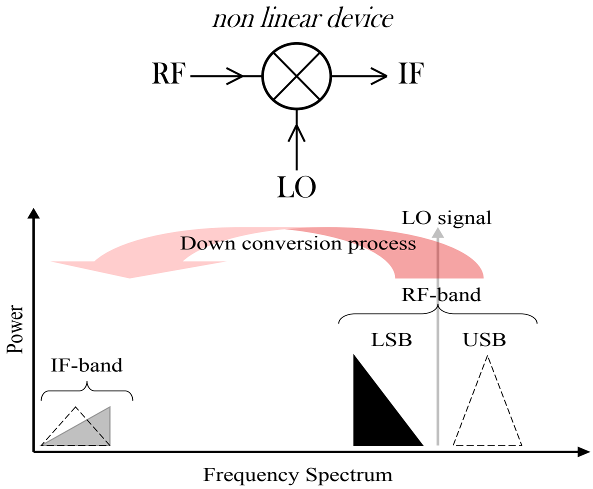

Fig. 2.3: System level circuit schematic of a mixer (top) and principle of the frequency downconversion process (bottom) of a fundamental mixer.

$$L_M = \frac{P_{RF,in}}{P_{IF,out}} \tag{2.9}$$

In resistive diode mixers it is the non-linear voltage-current characteristic of the diode that causes frequency mixing (intermodulation). A resistive switch, variable from zero Ohm's to infinity, makes a good first approximation of a resistive diode that is pumped by a large LO signal. Such an ideal mixer has a theoretical conversion loss of 6 to 3.9 dB assuming an ideal sinusoidal to square conductance waveform [77] with all frequency components terminated in a matched load.

In this analysis, the degradation factor of the conversion efficiency, due to non ideal switching in the real case, is found as the square of the difference between the maximum and minimum reflection coefficient for the two switching states, and is estimated to about 1 dB.

For Schottky diode mixers, degradation of the conversion efficiency is mainly due to the series resistance R_s and parasitic capacitance. In [78, 79] an analysis is made of this additional parasitic conversion loss predicting a minimum parasitic conversion loss contribution of 1 dB at 300 GHz to 4 dB at 1.5 THz.

Mixer conversion loss and equivalent input noise are the two main figure-of-merits for mixers. For submillimetre wave applications the lack of efficient and powerful LO sources, makes the mixer LO power requirement important as well. Other important parameters are conversion loss flatness and spurious generation. For image rejection (IR) mixers, IQ-mixers and sideband separating mixers (2SB mixers) the IR, phase and amplitude imbalance and sideband ratio SBR respectively are also important.

The concept of using an antiparallel diode pair for subharmonic mixing, was proposed by Cohn in 1975 [62], with a noise performance similar to fundamental mixers but requiring an LO at only half the RF frequency. The antisymmetric IV-relationship of an antiparallel diode pair causes the suppression of even harmonics when pumped by a LO signal. Since the antiparallel diode pair conducts current in both directions, i.e for the positive and negative periods respectively of an applied sinusoidal LO voltage, the small RF signal will see a conductance time domain waveform with half the period of the LO signal, which is the fundamental principle behind subharmonic mixing. Depending on circuit design any even order harmonic of the LO can be utilised for downconversion, and for an ideal perfectly balanced diode pair only odd order LO harmonics will be generated outside the diode loop. Currents containing the even harmonics are confined within the diode loop and canceled outside the diode circuit.

2.4 Schottky diodes

The name Schottky diode has been awarded Walter Schottky for his pioneering work during the 1930's and 40's in the field of metal-semiconductor interfaces [80]. However the discovery of the rectifying effect of a metal to semiconductor transition goes as far back as to 1894 and experiments conducted by Ferdinand Braun on metal-sulfides [81]. The Schottky-barrier model proposed by Cowley and Sze [82,83], explains many of the characteristic phenomenons seen in Schottky rectifiers. It includes the effects of surface states in the metal-semiconductor junction, first pointed out by Bardeen [84], and the effect of image-force lowering of the barrier, also known as the Schottky effect.

When a semiconductor and metal with different electron affinity are brought together, a potential barrier is created. The part of the semiconductor closest to the metal interface becomes depleted from charge carriers, leaving behind atoms with a net charge compensating for the potential difference until equilibrium is reached. The difference in potential between the conduction band and barrier height is called the built in junction potential. For GaAs Schottky mixer diodes, the rule of thumb when deciding on the epilayer thickness is that it should be around one depletion width at zero bias. The depletion width is given by:

$$w = \sqrt{\frac{2\epsilon_s(\phi_b - V_j)}{qN_d}} \tag{2.10}$$

with N_d being the epitaxial layer doping concentration, V_j being the voltage across the junction, ϕ_b the built in junction potential and ϵ_s the dielectric permittivity of GaAs. The two main current transport mechanisms of GaAs Schottky diodes are the thermionic emission and tunneling. By applying a positive forward voltage (positive at metal interface), the effective electron barrier height is lowered allowing for electron transport to the metal

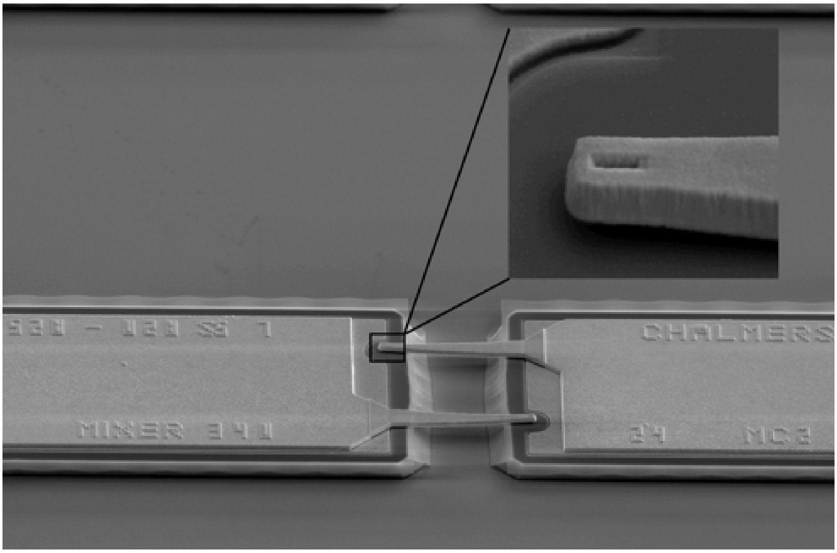

Fig. 2.4: Scanning electron micrograph of an antiparallel Schottky diode with a 0.44 μm^2 area. The devices have been fabricated at Chalmers University of Technology.

via thermionic emission. The exponential characteristic with respect to electron energy distribution in the semiconductor gives rise to a highly non-linear relationship between the forward current and applied voltage over the barrier:

$$I(V) = I_S(e^{\frac{q(V-IR_s)}{\eta k_B T}} - 1) \tag{2.11}$$

in which the reverse saturation current I_s is given by:

$$I_S = AA^*T^2 e^{-\frac{q\phi_b}{k_B T}} \tag{2.12}$$

with A being the area, A^* the effective Richardson constant, R_s the series resistance, η the diode ideality factor, k_B the Boltzmann constant and T the junction temperature.

The second transport mechanism is related to quantum effects allowing for tunneling of electrons through the barrier, which is a process independent of temperature. The tunneling current increases with decreasing barrier thickness and is not so pronounced at forward bias. However becomes important in backward bias direction e.g. as in varactor multipliers.

In Fig. 2.5 an electrical circuit representation of the intrinsic diode is shown. The effect of the parasitic series resistance is that less power is coupled into the Schottky junction increasing the conversion loss. For resistive mixers it is the non-linear resistance-voltage R-V relationship in the forward direction that is used for mixing. For varactor multipliers it is the non-linear junction capacitance-voltage C-V relationship for the reversed biased diode

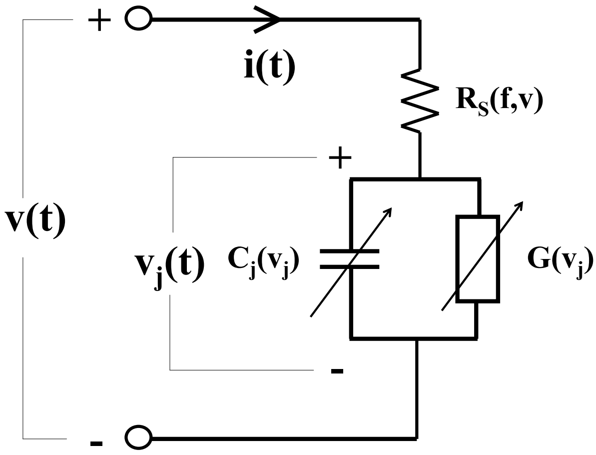

Fig. 2.5: Equivalent circuit model of the Schottky diode consisting of a resistance in series with a varistor and varactor in parallel.

that is utilised for harmonic generation. The voltage dependent junction capacitance is given by:

$$C_j = A\sqrt{\frac{qN_d\epsilon_s}{2(\phi_b - V_j)}} \tag{2.13}$$

Today GaAs Schottky diodes are commonly used for multiplier and mixer applications. Such devices are well suited for high-speed operation with reported cut-off frequencies reaching several THz. In Fig. 2.4 a scanning electron microscopy (SEM) image of a modern planar air-bridged antiparallel Schottky diode is shown. The diode intrinsic cut-off frequency f_c is defined as the frequency at which the magnitude of the reactance $\frac{1}{\omega C_j}$ equals the diode series resistance R_s:

$$f_c = \frac{1}{2\pi R_s C_j} \tag{2.14}$$

For high frequency operation, it is necessary to decrease the capacitance. The capacitance can be decreased by choosing a smaller anode size or by choosing a lower doping concentration for the epitaxial layer. Both will lead to a higher series resistance. Thus we have a trade off in noise performance and bandwidth [85]. There are three main contributors to the diode intrinsic series resistance:

$$R_s = R_{epi}(v_j) + R_{spread}(f) + R_{ohmic} \tag{2.15}$$

with R_{epi} being the effective resistance coming from the undepleted part of the epilayer, R_{spread} being the contribution of the spreading resistance [86] in the highly doped contact layer, and R_{ohmic} being the ohmic contact series resistance. Conductor losses in the diode package, e.g. coming from surface roughness and skin effect, can be included in the series resistance as well.

Optimisation of the Schottky barrier and parasitics is crucial for submillimetre frequency operation. Epilayer thickness, doping concentration, contact size and layout have to be optimised. The diode ideality and noise characteristics heavily depend on the quality of the Schottky contact and epitaxy. The contact formation involves deposition of different metals, e.g. Ti/Pt/Au for evaporated contacts and Pt/Au for pulse plated contacts, on top of a preconditioned semiconductor epitaxial layer surface. The doping concentration for high frequency diodes is chosen rather high, in order to reduce the series resistance coming from the undepleted region of the epilayer. However choosing a too high doping level will often lead to an increased ideality factor, increasing the leakage current and shot noise.

When it comes to the realisation of modern THz Schottky diodes used for THz detectors and sources, planar air-bridged devices [39] are used owing to there ability to withstand stress, there superior repeatability and ease of assembly. Moreover, planar technology enables simple realisation of complex diode structures such as anti-parallel, anti-series and in-series diode configurations used in subharmonic mixers, balanced mixers and multipliers etc. The extrinsic diode parasitics can be modeled as a pad-to-pad capacitance, a finger inductance and finger capacitance [87]. The parasitic finger capacitance is closely linked to the process capability. A lumped schematic model of an anti-parallel diode and its 3D layout correspondence is shown in Fig. 2.6. The highly doped conductive contact layer (buffer layer) shown in red has been tapered for minimising the pad to pad capacitance. Device modeling and parameter extraction requires some kind of lumped device model. The lumped model can also be used for circuit design and optimisation of the diode structure. In general the simpler the model i.e. less number of components in the model, the easier it is to fit measurements and simulations. However for accurate prediction of higher order effects, such as proximity effects, eddy currents and skin effect [88], which become more pronounced at higher frequencies, more advanced models have to be used [89, 90].

2.5 Noise theory

The noise in Schottky diodes has been the subject of extensive study. The two main noise mechanisms that contribute to the diode's intrinsic noise are the shot noise and thermal noise [91]. The excess noise or hot noise is the measured noise that can not be explained by the shot noise and thermal noise models.

The shot noise is due to the discrete nature of electrons and random variations of the electrons passing through the barrier. The mean squared shot noise current in the diode junction, modeled as a shunted current source, is given by [73, 74]:

$$\langle {i_{shot}}^2 \rangle = 2qIB \tag{2.16}$$

with B being the bandwidth and I the current through the junction. Thermal noise (also called Johnson or Nyquist noise) originating from the diodes series

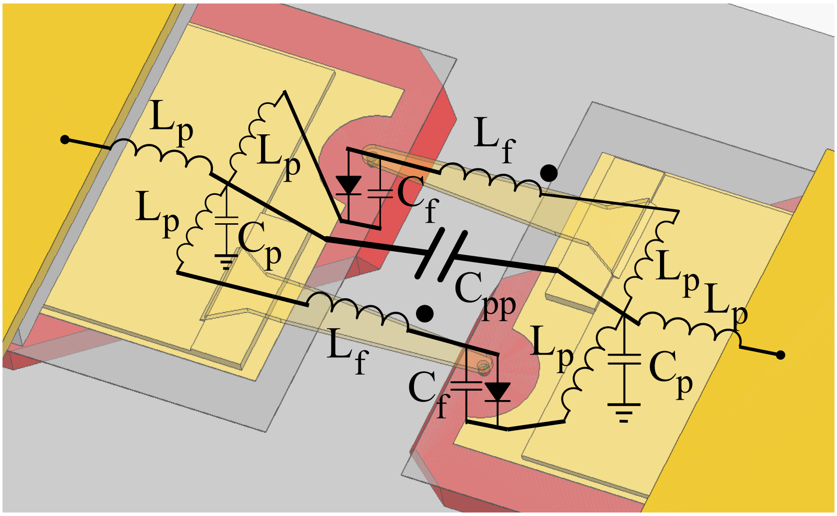

Fig. 2.6: Lumped model represantion of the anti-parallel planar diode with mutual inductive coupling between fingers [89] on top of a 3D-EM model with internal lumped ports replacing the diodes, the highly doped conductive buffer layer is shown in red.

resistance is together with shot noise a major noise contributor in room temperature applications. The thermal noise depends on the device temperature. It can be modeled as a voltage noise source in series with the corresponding series resistance with a mean square voltage given by [92, 93]:

$$\langle v_n^2 \rangle = 4k_B BTR \tag{2.17}$$

The excess noise e.g. hot electron noise and high field noise, which is due to a non-equilibrium distribution of electrons in the conduction band and scattering effects, will come into effect at high current distributions. Furthermore it will like the shot noise have a cyclostationary character i.e. it will vary over the LO pump cycle. The excess noise can be estimated empirically and by looking closer into the the electron transport mechanisms and operation of the mixer diode [94, 95].

Chapter 3

Mixer design

This chapter deals with the general aspects of waveguide integrated designs. The design of a subharmonic 340 GHz Schottky mixer using hybrid technology is presented. The 2SB mixer design is briefly discussed and results are presented.

3.1 Design methodology

An iterative "divide and conquer" design approach is adopted, breaking up the circuit in parts, where each part is simulated and optimized individually. The different parts are then combined and and optimised together. The combining process has an iterative nature, see Fig. 3.1.

3.2 Circuit technology considerations

The choice of circuit topology is important and mainly decided by the technologies that are at hand. Submillimetre wave circuit implementations range from the simpler and less expensive hybrid circuit topologies, in which typically low dielectric and low loss materials, e.g. quartz are used together with discrete diode components that are "flip chip" mounted/soldered to the circuit, to ultra thin ($\sim \mu$m) membrane MIC structures with an arsenal of circuit features such as beam leads, on chip resistors and capacitors and air-bridges. In between we find circuit technology hybrids such as quartz circuit carriers with beam leads and with integrated active components using substrate transfer techniques, and MMIC's that have been diced and mechanically thinned to fit the waveguide assembly.

For the 340 GHz mixer the goal was to make a design based on commercially available technology i.e. fabricated to a low cost, why a hybrid circuit design using discrete diodes was chosen as the baseline. To simplify assembly and assure good repeatability of ground connections a suspended inverted mixer topology was chosen for the design, similar to [36]. Suspended topologies are less sensitive to substrate thickness variation, compared to microstrip circuits, however are more sensitive to variations in width.

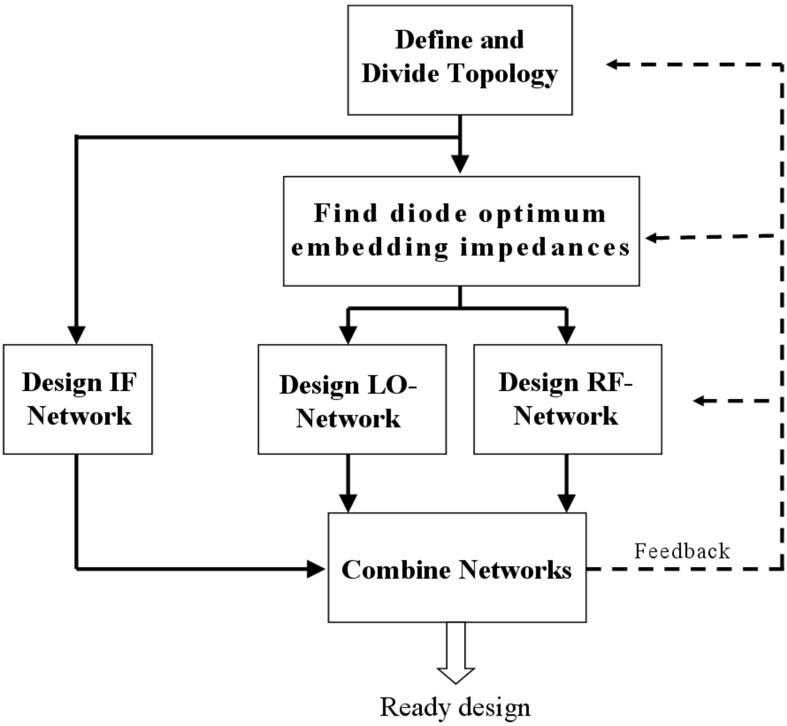

Fig. 3.1: Mixer design process flow chart.

3.3 Subharmonic (x2) mixer topologies

Fundamental single ended mixers require some kind of RF/LO combiner, a topology that can become both lossy and bulky. The subharmonic x2 mixer uses half the effective LO frequency. This allows for a natural separation of the RF and LO ports, which simplifies the circuit design considerably. For fundamental mixers, balanced topologies can be used instead.

An anti-parallel diode mixer configuration can be implemented in two ways, see Fig. 3.2. The main difference of these two topologies is that the RF and LO choke filters have to provide a short circuit in one case and an open circuit in the other.

The series connected antiparallel-diode configuration is more suitable for high frequency operation as it does not require a ground connection, which the shunt connected antiparallel-diode configuration does. The shunt connected antiparallel-diode mixer topology can also be implemented using a series pair with the center node connected to the signal strip and with the outer nodes grounded. This topology becomes interesting for TMIC designs in which the individual diodes can be biased [96].

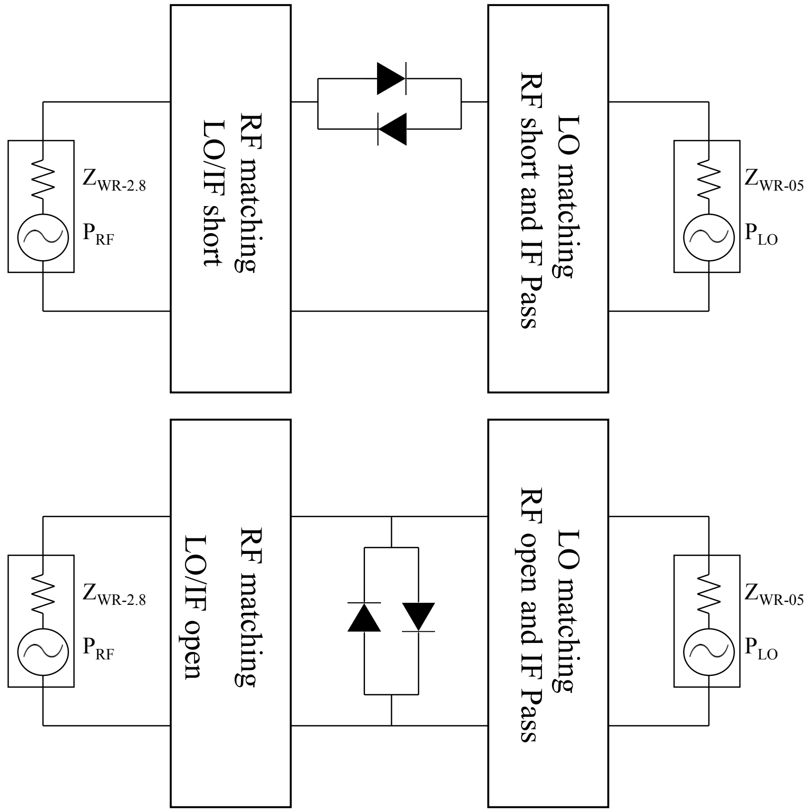

Fig. 3.2: Schematic of series (top) and shunt (bottom) type mixer topologies employing antiparallel diodes. The IF port is embedded in the LO port.

3.4 E-field coupled rectangular waveguide to planar transmission line transitions

Supporting only one polarisation, the rectangular waveguide with a 2:1 aspect ratio, is by far the most common waveguide type used in submillimetre wave systems. Waveguide probes are used to efficiently couple power between the planar circuit and the fundamental TE_{10} mode of the rectangular wavwguide. The planar circuit is typically situated inside a shielded channel and can be of microstrip, suspended stripline or coplanar waveguide type. By extending only the signal strip out in the waveguide an electric field probe (E-Probe) is created. The shape and length of the E-probe is typically co-optimised with a waveguide backshort and close to 100% coupling efficiency can be realised almost over a whole waveguide band. The mechanical design of a waveguide transition can be realised in many ways. In the case that the waveguide is split along the H-plane symmetry, we get a E-plane splitblock. The E-plane splitblock type is the most common and also gives the lowest loss as none of

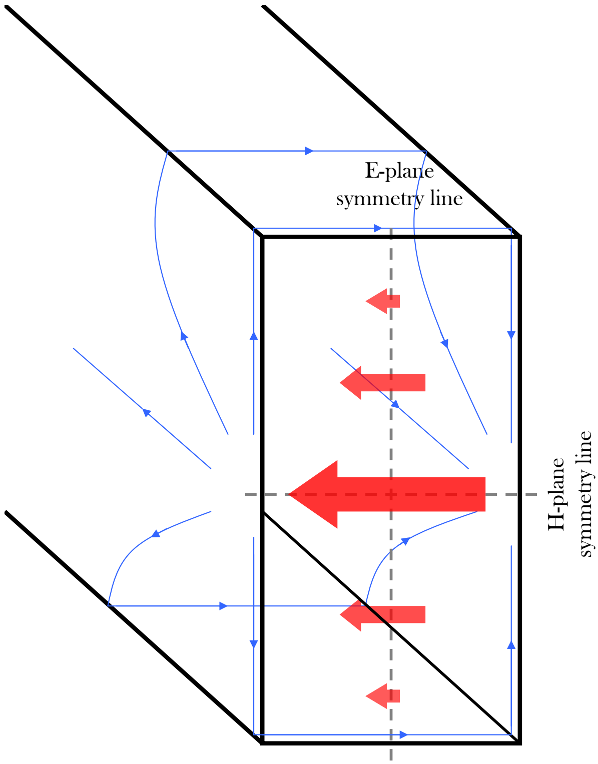

Fig. 3.3: Rectangular waveguide showing electric field (red arrows) and surface currents (blue) on the guide walls for the TE_{10} mode. The H-plan and E-plane symmetry lines are also indicated.

the currents of the waveguide mode are broken. It also has the advantage of high flexibility in terms of embedding other components.

When no additional functionality is needed a single open-ended E-field probe can be used. If a DC or out of band ground connection is needed a planar backshort can be used similar to the RF probe seen in Fig. 3.9. The extended transmission line backshort can be replaced by a RF choke filter providing an alternative connection port at lower frequencies, see Fig. 3.7. Full height waveguides or reduced height waveguide with larger tuning capability can be used.

These are the most common types, thereto a large variety of different probes exists e.g. H-plane probes and differential probes [97–102].

3.5 Planar filter structures

The most common planar choke filter is probably the stepped impedance filter with alternating low and high impedance quarter wavelength long sections, see Fig. 3.7 and Fig. 3.8. This filter topology offers a very good rejection to a relative few number of sections. The main advantage of this filter, besides that it is extremely simple to design, is its minimum lateral extension, which is typically needed for waveguide embedded shielded circuit topologies. The disadvantage is the length of the filter. Another alternative to the stepped impedance filter is to use the more complex hammerhead filter topology or curved open stubs for which coupling effects have to be considered.

In general wire bonding is to imprecise to be used at frequencies above 300 GHz. One alternative is to manually solder the gold wires in a similar fashion as the soldering of the diode chip, however this is not advantageous from a repeatability and production perspective. Grounding vias are difficult and expensive to fabricate for substrates thicknesses below 100 μm. Hybrid technology is thus limited to circuit implementations that do not depend on accurate grounds and circuit interconnects.

The best way in terms of reproducibility and ease of assembly is probably to use beam leads that are clamped in between the two split blocks. However beam lead technology requires a process in which the substrate carrier is etched away. Both quartz circuits and GaAs circuits can be manufactured with beam leads by etching and/or lapping techniques. A low cost alternative to the more process extensive beam lead technology is to suspend the substrate in an inverted position. The suspension points can then be used for RF and DC interconnects using conductive glue or soldering.

Another useful and simple filter with minimum lateral extension is the coupled line filter. Multi-section coupled line filters however typically suffer from high transmission losses and should therefore be avoided.

3.6 3D-modeling of diodes

To be able to accurately predict the diode chip optimum embedding impedances a full 3D electromagnetic (EM) simulation of the diode in its circuit environment is necessary. In Fig. 3.4 the 3D model of the diode package is shown. In the simulation the diode pad interfaces are extended, and the reference plane of the transmission line wave ports are later de-embedded back to the diode reference planes. This is done not to excite evanescent modes at the port interfaces. The active part of the diode is replaced by an internal coaxial [87] or lumped port. In this way the diode barrier (non-linear part) and diode parasitics (passive 3D part) can be separated.

The result of the 3D-EM simulation is imported in the form of a S-parameter file and the internal ports are connected to a non-linear diode model. The diode component is connected from the internal ports down to ground. Important to keep in mind is the phase of the port and diode in

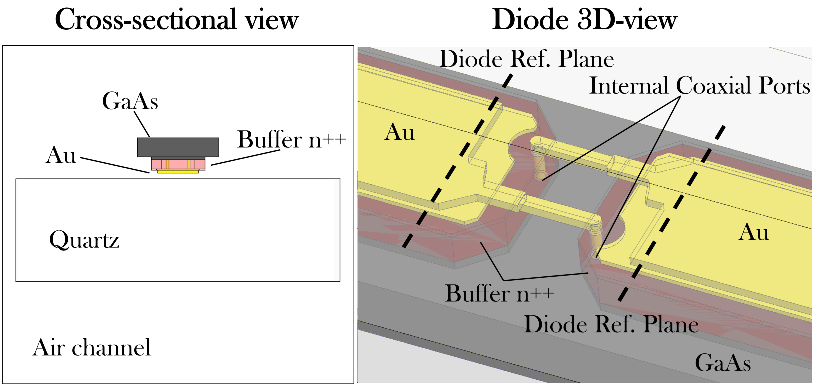

Fig. 3.4: Full 3D-Model used for EM simulation of the flip-chip mounted antiparallel diode chip.

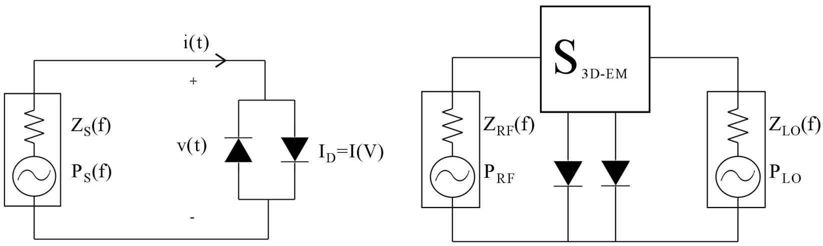

Fig. 3.5: Principle HB simulation setup of the aniparallell diode mixer topology, ideal case (left) and combining 3D-EM simulations of the diode chip.

order to get the antiparallel configuration right, see Fig. 3.5. By using a load pull technique and harmonic balance simulations, the optimum conversion loss RF, LO and IF diode embedding impedances can be found. Frequency dependent source impedances are used to terminate intermodulation products. Different simulations schemes, applying perfect ground (ideal), open or 10 Ohm (average real) for the spurious terminations can be used to study the impact on the optimum embedding impedances and performance. In Fig. 3.6 the embedding impedances for an ideal diode are compared to the embedding impedances of the diode chip. A practical approach for designing a mixer is to aim for low conversion loss maintaining the lowest possible LO power ensuring a low current density through the diode and thus low shot noise.

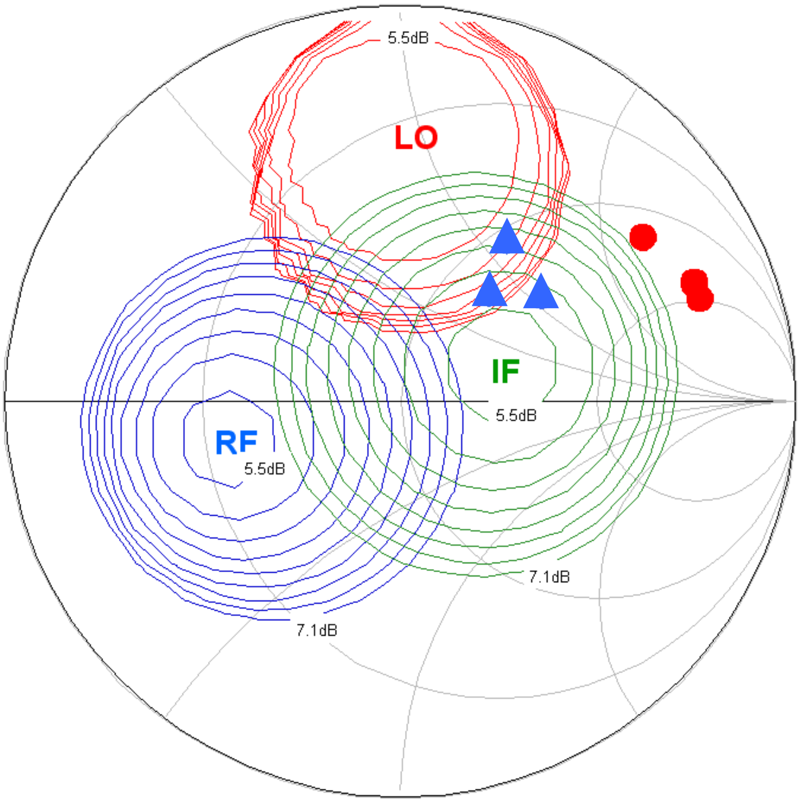

Fig. 3.6: HB load pull simulations at 170 GHz and 340 GHz LO and RF frequency respectively, showing the optimum RF (triangles) and LO (circles) conversion loss diode embedding impedances comparing to the results in [36, 87]), for an ideal diode with $R_s = 13\ \Omega$, $C_{j0} = 1.5$ fF and $\eta = 1.3$. Conversion loss contour plots from 5.5 dB to 7.1 dB in 0.2 dB steps using a full 3D diode model and diode parameters $R_s = 8\ \Omega$, $C_{j0} = 3.5$ fF and $\eta = 1.2$. The system impedance is 50 Ω.

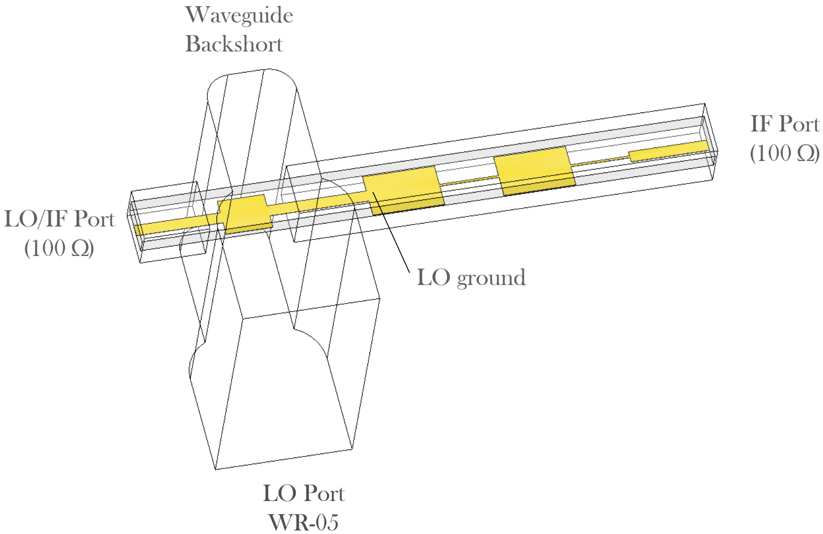

Fig. 3.7: Full 3D-Model used for EM simulation of the complete LO/IF duplex filter.

3.7 LO/IF filter circuit

The design of the LO/IF duplex filter is presented in Fig. 3.7. The LO-IF diplexer can be divided into three parts, partial design of a symmetrical LO probe (to WR-05), design of a planar LO choke filter, and final co-optimisation of the two. The characteristic system impedance is defined by the transmission lines. In this case 100 Ω was chosen as it gives realisable line widths for the stepped impedance filter and simultaneously work as an impedance transformer from the mixer IF impedance, which is typically above 150 Ω, to the 50 Ω input of the LNA.

3.8 LO matching circuit

Once the diode chip optimum embedding impedances are found the design of the matching circuits can begin. The LO matching circuit should also provide a ground for the RF signal at the diode reference plane. Thus it has two satisfy two conditions which is the main challenge of the design. For the case of a broadband RF and narrowband LO, a RF choke filter topology with a low impedance section directly at the diode chip can be chosen, see Fig. 3.8. It will give the most broadband RF response, and the remaining sections can then be optimised to match the LO. The LO probe can also be utilised and be a part of the LO matching. The diode chip interface has been included in the simulation and extended for suppression of evanescent modes. The diode wave ports are later de-embedded to the correct diode reference position.

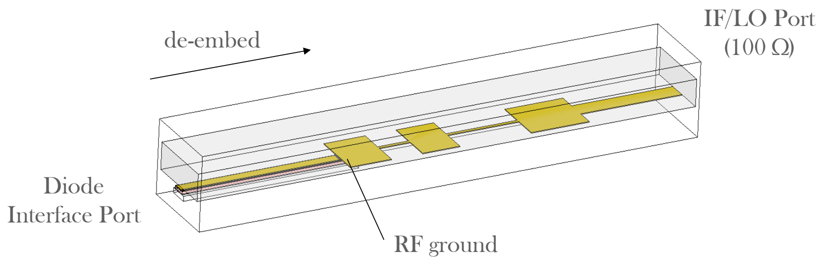

Fig. 3.8: Full 3D-Model used for EM simulation of the RF ground/ LO matching circuit.

3.9 RF matching circuit

The RF matching circuit contains both planar circuitry, as the diode is positioned inside the mounting channel and a 3D waveguide part using a reduced height waveguide (WR-2.8), see Fig. 3.9. Moreover a planar backshort is used for the realisation of the IF and LO ground. The microstrip ground (planar backshort) is transformed back to a short circuit at the diode interface. The reduced height not only works as an extra matching section for the RF matching network, but also reduces the distance between the planar short and the diode chip. The diode chip interface has been extended and the port is later de-embedded to the diode reference plane.

3.10 Mixer circuit design and results

When all subcircuits have been optimised the complete mixer is simulated and final tweaks can be made, see Fig. 3.13. The S-parameters of this simulation can then be plugged into the HB-simulation. The designed matching circuits reflection coefficients are presented in Fig. 3.14 on top of the optimum conversion loss contours. A typical simulated response of the mixer is presented in Fig. 3.10 and in Fig. 3.11.
In Fig. 3.12 a fabricated fuzed quartz mixer circuit side by side with a Schottky diode chip is shown.

3.11 CW conversion loss measurements

For verification of the conversion loss measurements using the Y-factor method, a CW measurement was done. The output of a multiplier chain was directly connected to the RF port of the mixer. The measured conversion loss over RF frequency for two different LO frequencies is presented in Fig. 3.15. The moving average of the two curves goes from about 8 dB to 12 dB with a maximum peak to peak ripple of 7 dB. The ripple points to a large RF standing wave affecting the accuracy of this measurement. By changing the test setup

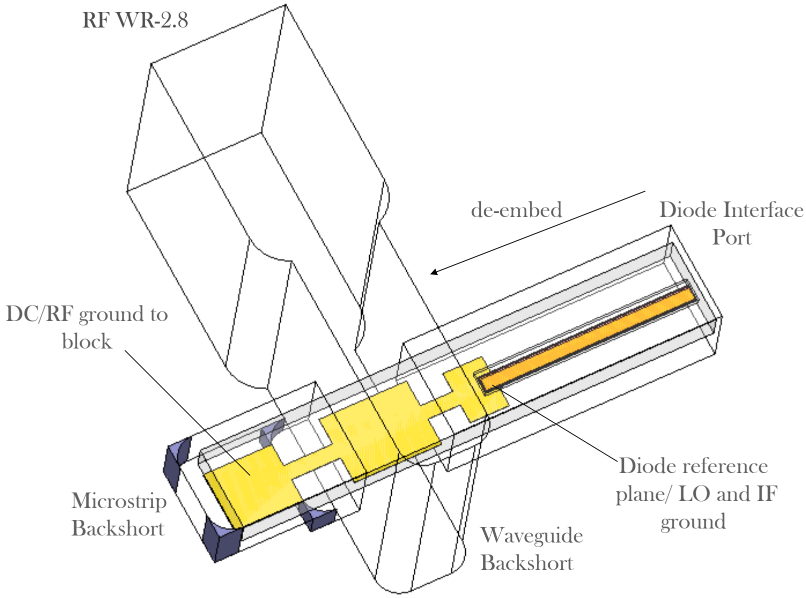

Fig. 3.9: Full 3D-Model used for EM simulation of the LO/IF ground/ RF matching circuit.

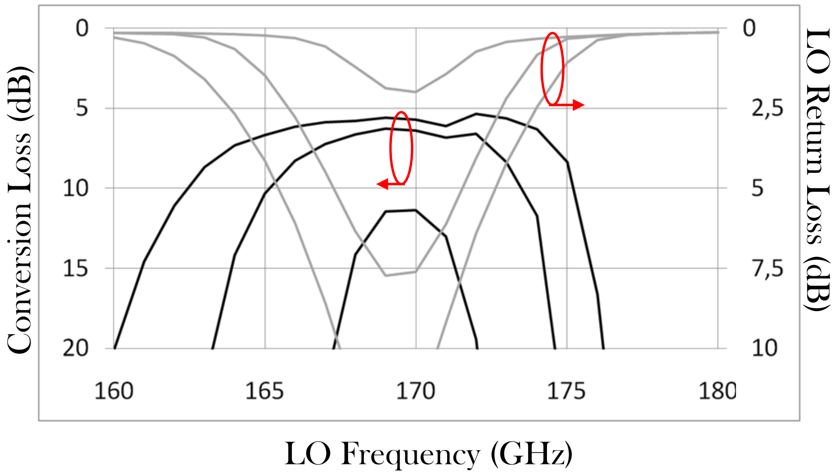

Fig. 3.10: Simulated mixer conversion loss and LO return loss at 2 GHz IF frequency over LO frequency, at 0.5 mW, 1 mW and 1.5 mW LO drive respectively. The simulated diode area is about 0.8 μm^2 and the simulation is based on a full 3D-EM model of the mixer using ideal conductors.

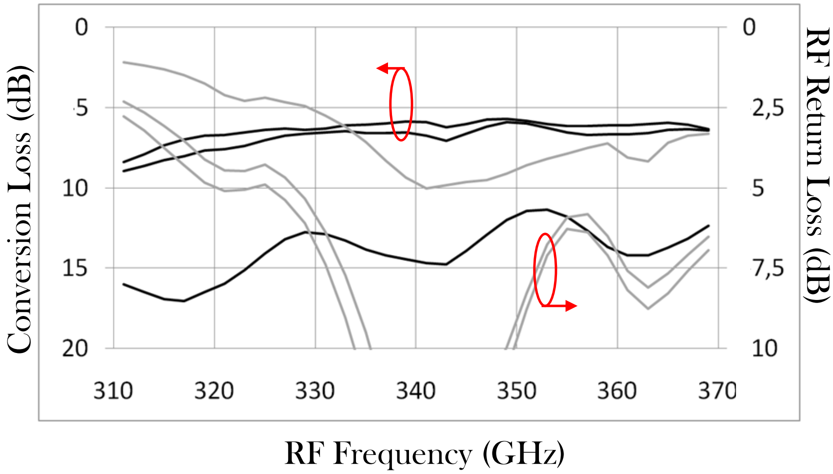

Fig. 3.11: Simulated mixer conversion loss and RF return loss over RF frequency, at 0.5 mW, 1 mW and 1.5 mW LO drive respectively and with fixed LO frequency at 170 GHz. The simulated diode area is about 0.8 μm^2 and the simulation is based on a full 3D-EM model of the mixer using ideal conductors.

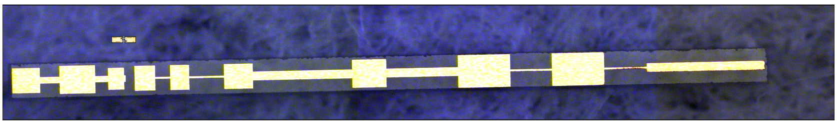

Fig. 3.12: Photograph of a 340 GHz mixer quartz circuits fabricated at Chalmers University of Technology. The mixer circuit is about 5 mm long 240 μm wide and about 70 μm thick. A discrete diode chip has also been inserted to the picture for comparison.

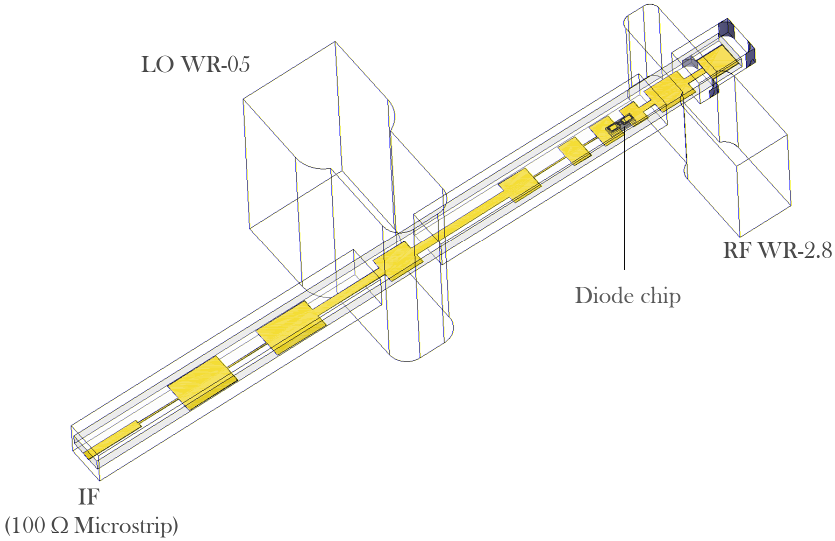

Fig. 3.13: Full 3D-Model used for EM simulation of the complete mixer design.

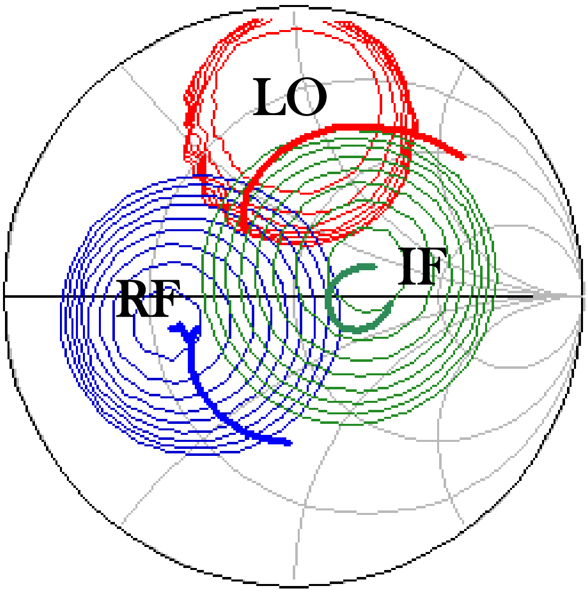

Fig. 3.14: Equivalent reflection coefficients of the RF, LO and IF matching circuits seen by the diode at the diode chip reference plane. The RF, LO and IF simulated frequency range is about 310-370 GHz, 160-180 GHz and 0-20 GHz respectively. The system impedance is 50 Ω.

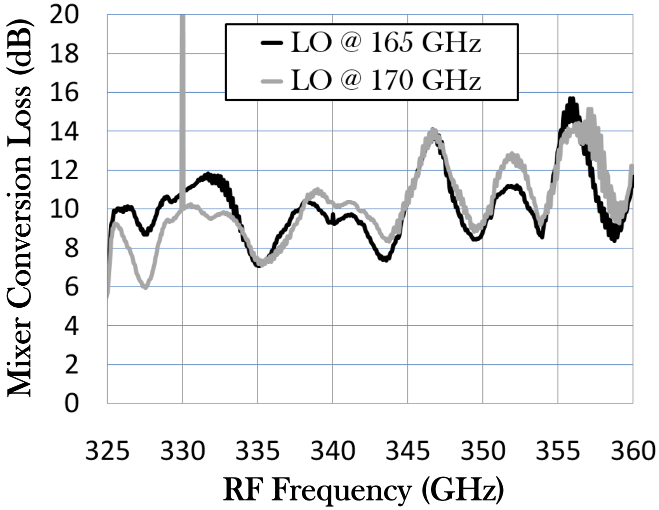

Fig. 3.15: Measured conversion loss at 160 GHz and 170 GHz LO frequency using a RF CW source.

to include an isolator, directional coupler or attenuator the RF standing wave could potentially be reduced improving the accuracy of this measurement method.

3.12 IQ Mixer design

The IQ-mixer constitutes the core of the 2SB receiver architecture. IQ stands for in-phase quadrature-phase referring to the 90 degree phase difference between signals. An IQ mixer can either be realised by introducing an effective quadrature phase difference in the LO or RF feeding. By connecting the two I and Q IF signal outputs to a quadrature scheme, the upper and lower sidebands can be separated. The individual I and Q signals contain phase correlated downconverted USB and LSB signals. The relative phases of these IF signals are defined by the RF and LO hybrid phase difference, together with the downconversion process in the mixer, which can be fundamental or harmonic. In the harmonic case the LO hybrid phase difference will be multiplied by the harmonic of the mixer. In Fig. 3.16 the relative phases of the USB and LSB signals propagating through an ideal 2SB receiver circuit are shown. The details of the developed low VSWR 2SB receiver design are described in paper [A].

In one of our first experiments on a modular 2SB receiver prototype the image rejection could be improved from about 5-10 dB to 20 dB by a simple linear phase compensation. The phase compensation was done in 3 GHz bands using two mechanical phase tuners inserted in the I and Q paths and

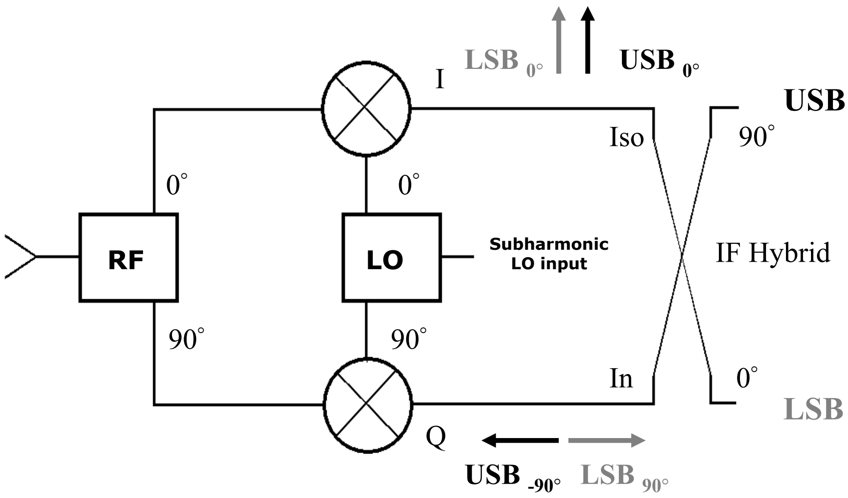

Fig. 3.16: Schematic of the subharmonic 2SB receiver topology based on RF and LO quadrature feeding.

the result is presented in Fig. 3.17. A simple amplitude tuning could be applied by using fixed IF attenuators of equal length or by switching LO feeding port at the LO hybrid. However the main unbalance seem to be in phase, with up to 60 degrees of compensation needed.

In Fig. 3.18 the IQ-mixer test setup is shown. A WR-05 waveguide had to be used between the IQ-mixer and commercial doubler because of the tight spacing between the LO hybrid ports.

In paper [A] the characterisation of the waveguide integrated low VSWR 2SB receiver is presented in detail. The assembly of the 2SB receiver is shown in Fig. 3.19.

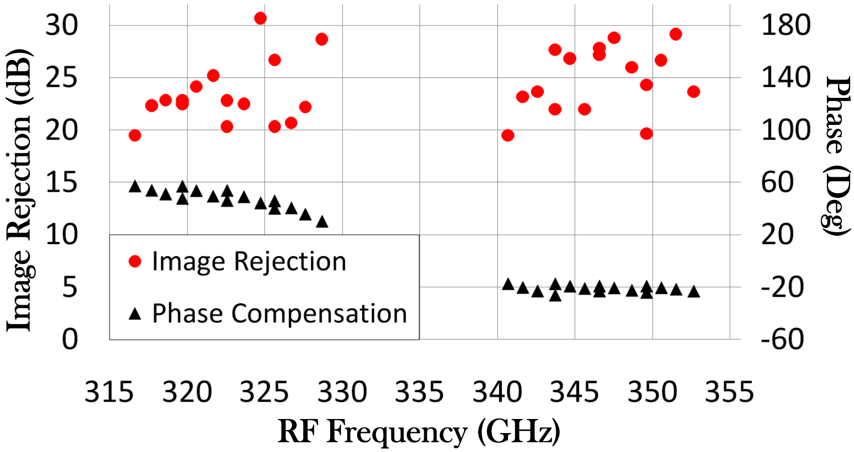

Fig. 3.17: Measured image rejection at 168 GHz LO frequency, using first order phase compensation in 3 GHz IF bands.

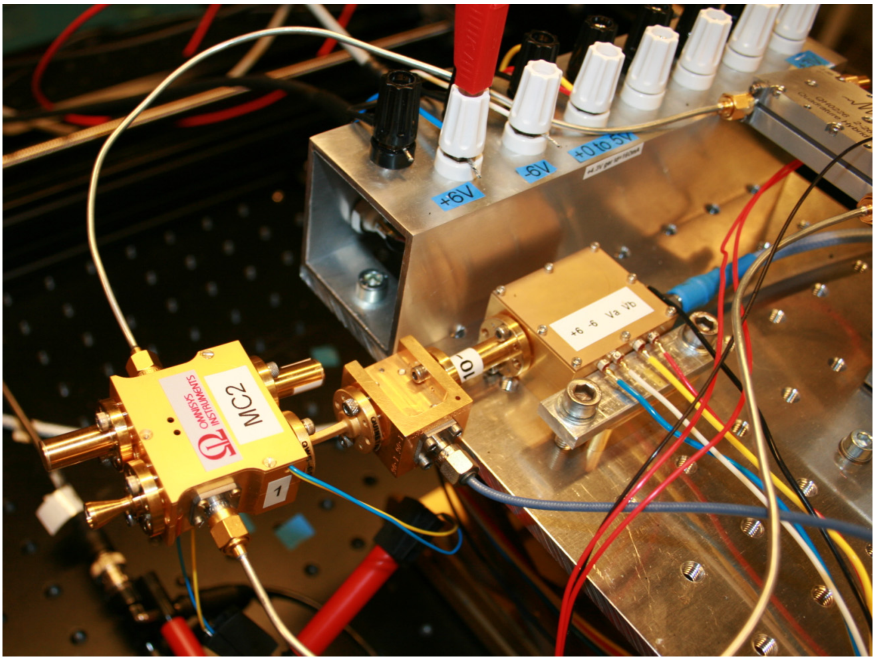

Fig. 3.18: Test setup for characterisation of the IQ-mixer.

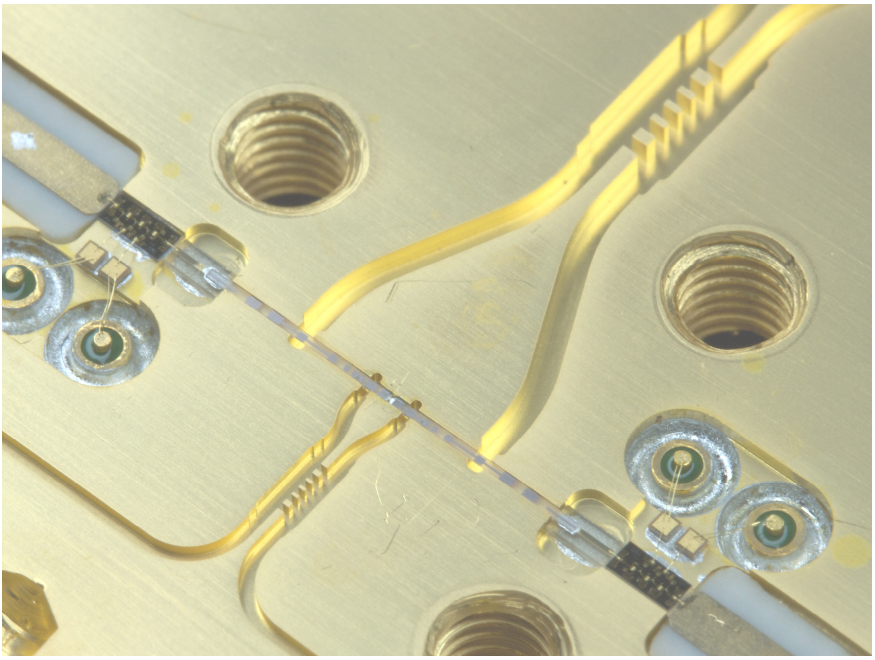

Fig. 3.19: Assembly of the low VSWR IQ-receiver consisting of two branch guide couplers, two with embedded LNA's.

Chapter 4

Y-factor measurements

The receiver noise can be measured by simply looking at the ratio in detected noise power P_H and P_C using a matched RF termination at two different and known physical temperatures, corresponding to the equivalent brightness temperatures T_H and T_C respectively. This is the principle of the Y-factor measurement method [91], [103]. By using (2.2) the Y-factor can be written as:

$$Y \equiv \frac{P_H}{P_C} = \frac{(T_R + T_H) \cdot G \cdot k_B \cdot B}{(T_R + T_C) \cdot G \cdot k_B \cdot B} \tag{4.1}$$

with T_R being the equivalent receiver input noise not saying that the receiver is of DSB or SSB type. We see that the Y-factor is independent of bandwidth B and gain G, that are assumed to be the same for the two measurements, and only depends on the hot and cold load temperatures. (4.1) is simplified to:

$$Y = \frac{(T_R + T_H)}{(T_R + T_C)} \tag{4.2}$$

For the case of a DSB receiver T_R is defined as the equivalent receiver DSB noise temperature and in the case of a SSB receiver it is defined as the receiver SSB noise temperature. Another way of viewing (4.2) is by rewriting it for the case of an ideal DSB receiver having a SBR equal to 1:

$$Y = \frac{(T_{R,SSB} + 2 \cdot T_H)}{(T_{R,SSB} + 2 \cdot T_C)} \tag{4.3}$$

In the ideal case the DSB receiver SSB noise will be equal to two times the DSB noise and (4.3) becomes identical to (4.2). Comparing the DSB receiver case in (4.3) to the SSB receiver case using (4.2) the only difference is in the factor 2 in front of the hot and cold temperatures, which is a consequence of the DSB receiver detecting radiation coming from both sidebands in contrast to the SSB receiver which rejects the image band.
By solving (4.3) with respect to the unknown SSB noise temperature for the DSB receiver we get:

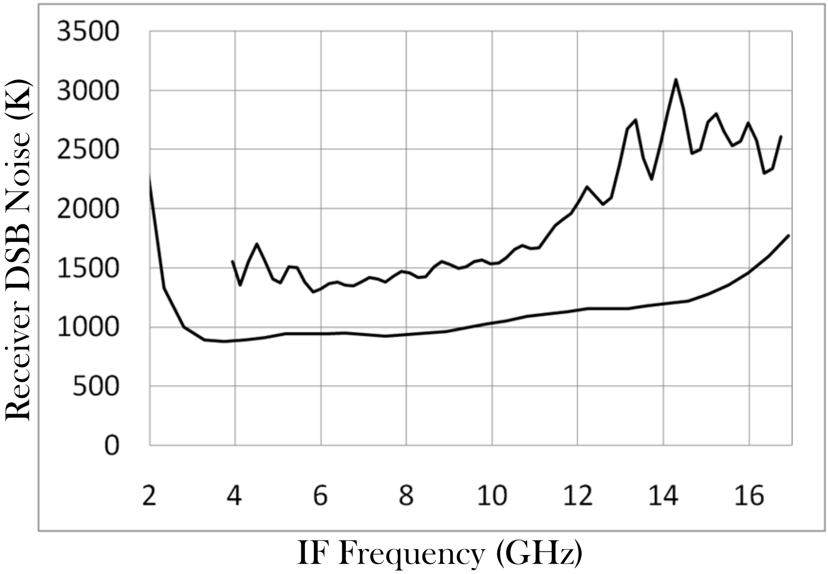

Fig. 4.1: Measured receiver noise for two mixers, one with an external LNA showing more ripple and higher noise and one with an embedded LNA.

$$T_{R,SSB} = \frac{2(T_H - T_C \cdot Y)}{Y - 1} \tag{4.4}$$

and for the SSB receiver case using (4.2) we have:

$$T_{R,SSB} = \frac{T_H - T_C \cdot Y}{Y - 1} \tag{4.5}$$

Again the only difference is the factor two comparing the DSB and SSB case.

In Fig. 4.1 the receiver noise over IF frequency for two different receivers using Y-factor measurements is shown. Both modules used the same mixer and LNA design however one of the mixers had the LNA embedded in the waveguide block, while the other used a coaxially packaged external LNA. The mixer with embedded LNA used commercially supplied diodes from VDI with typical diode parameters specified as; $C_{tot} = 7.5 - 10.5fF$, $R_{s,max} = 13\Omega$ and $C_{pp,max} = 3.5fF$. The mixer with external LNA used diodes with 0.8 μm^2 area fabricated at Chalmers, with diode parameters $C_{tot} = 11fF$, $R_s = 8\Omega$, $C_{j0} = 2.5fF$ and $\eta = 1.3$, and with a doping concentration $N_D = 5 \cdot 10^7 cm^{-3}$ and epilayer thickness $t_{epi} = 48nm$. The LNA equivalent input noise was 30 to 80 K in the 4-14 GHz band(50Ω). The LO frequency was around 170 GHz for both measurements. The difference in performance seen as an offset is mainly due to that different diodes are used. The IF mismatch is clearly shown for the receiver using the external LNA as a large ripple in the response.

Table 4.1: Receiver noise temperature T_R in Kelvin versus Y-factor in dB with T_{hot}=300 K (RT) and T_{cold}=77 K (LN) using (4.2)

Y [dB]	T_R [K]
0.1	9500
0.2	4650
0.3	3040
0.4	2230
0.5	1750
0.6	1430
0.7	1200
0.8	1030
0.9	890
1	780

In Table 4.1 values for the equivalent receiver noise temperature T_R in (4.2) for different Y-factors are found.

By adding an attenuator with loss L_{Att} at the ambient temperature T_{Amb} in between the mixer and the LNA, we can also determine the mixer equivalent noise temperature and conversion gain. The input noise temperature of an attenuator with loss L_{Att} equals to [91]:

$$T_{att} = T_{Amb}(L_{Att} - 1) \tag{4.6}$$

The input noise temperature for a 3 dB attenuator at room temperature is thus equal to 290 K. Placed in between the mixer and the LNA in a receiver system it also increases the contribution of the LNA input noise temperature to the output of the mixer by a factor of two. Using (2.8) and Friis formula, the DSB receiver input noise temperature can now be rewritten as:

$$T_{R,SSB,3dB} = T_{M,SSB} + L_{M,SSB}(T_{Amb}(L_{3dB} - 1) + L_{3dB} \cdot T_{LNA}) \tag{4.7}$$

with $T_{M,SSB}$ and $L_{M,SSB}$ being the mixer input SSB noise and SSB conversion loss respectively, T_{LNA} being the LNA input noise and L_{3dB} being the loss of the attenuator. By subtracting (2.8) from (4.7) we get an explicit expression for the mixer conversion loss as a function of the difference in measured receiver noise temperature and the LNA equivalent noise temperature.

$$L_{M,SSB} = \frac{T_{R,SSB,3dB} - T_{R,SSB}}{T_{Amb} + T_{LNA}} \tag{4.8}$$

The equivalent mixer input noise can be calculated by subtracting the IF noise contribution. However due to IF standing waves using the 50 Ω matched LNA input noise temperature will lead to a large error. There are many ways around this problem which all include additional characterization of the IF

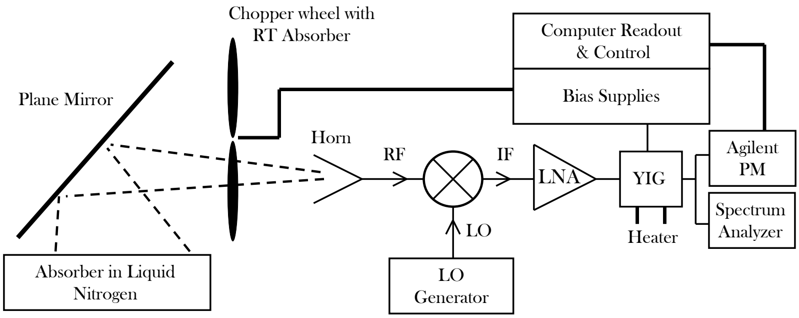

Fig. 4.2: Schematic of hot and cold load setup for Y-factor measurements.

mismatch in some way. For instance, by using an IF isolator with known loss the effect of standing waves can be eliminated. A directional coupler can be used to inject IF noise into the LNA including the effect of standing waves. By measuring the mixer IF impedance the mixer noise can be extracted only for those frequency points that are close to 50 Ω, or the LNA input noise can be estimated based on simulations including the measured IF impedance. In Fig. 4.3 a typical mixer measurement scenario using the Y-factor method can be seen.

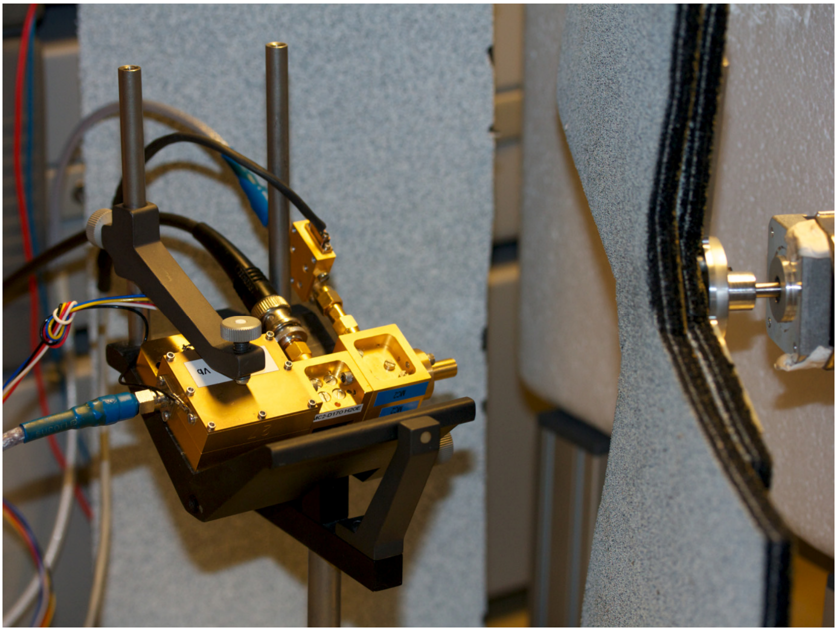

Fig. 4.3: Y-factor measurement of a DSB mixer with external LNA.

Chapter 5

S-parameter characterisation of TMIC devices and circuits

On wafer probing is typically used at microwave frequencies for the characterisation of MMIC and thinfilm devices and circuits using microstrip and coplanar transmission lines, with the advantage of being fast, accurate and simple. However due to coupling effects in between probes, the open boundary environment and difficulties in getting repeatable connections, on wafer measurements become challenging at millimetre and submillimetre wave frequencies and waveguide based calibrations are often used [104]. Today frequency extenders up to 1 THz are becoming commercially available [105]. On wafer measurements at such high frequencies call for novel probe interfaces [106] as well as new standards for the waveguide flange interfaces [107]. Moreover on wafer measurements become less representative for the operation of assembled/packaged THz components, e.g. membrane circuits, calling for complementary characterisation methods.

At submillimetre wave frequencies embedded and suspended circuits topologies are often used in close symbiosis with the package, e.g assemblies with waveguide interfaces. At these frequencies waveguide based measurements are often used based on the TRL-calibration technique. The method relies on a partially known imperfect 1-port reflect standard (open or short) and on the relative distance of two otherwise identical 2-port transmission guide standards (thru and line). Such standards are easily implemented in almost any guiding structure. By implementing the calibration standards embedded in a planar structure e.g on a waveguide embedded membrane circuit, it is in principle possible to characterise packaged membrane devices and circuits "on wafer", see Fig. 5.1.

However applying such a method directly violates a fundamental principle of microwave engineering; *"you shall not break the calibration path"* by at least 4 times. This is the main concern of the proposed method. The repeatability of the waveguide interfaces has to be considered as well as the repeatability of the waveguide probe interfaces, which includes machining tolerances, processing tolerances and assembly tolerances.

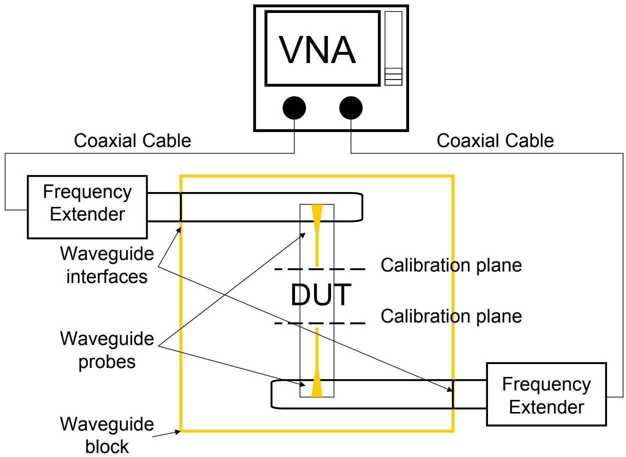

Fig. 5.1: TRL calibration and S-parameter characterisation of waveguide embedded membrane circuits.

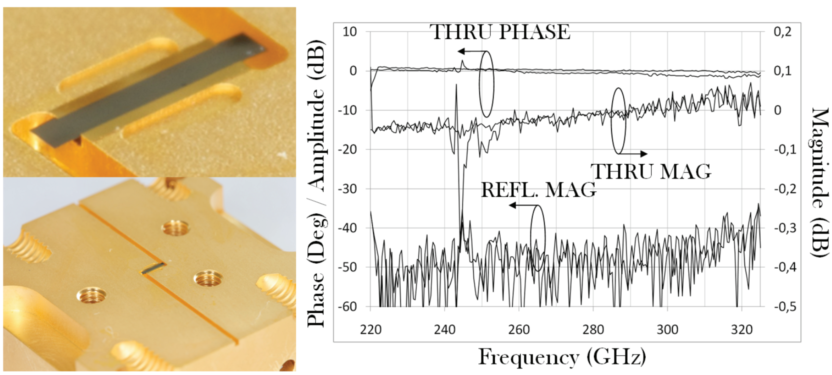

Fig. 5.2: Photo of an opened TRL-thru standard block and enlarged photo of the membrane thru circuit mounted with the circuit trace facing down. S-parameter data over the 220 GHz to 325 GHz frequency range showing the repeatability of the thru standard after reconnection of the waveguide interface.

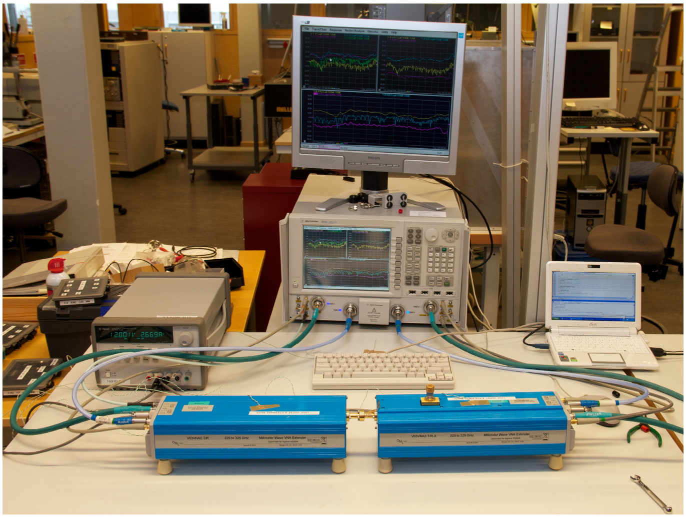

Fig. 5.3: S-Parameter measurement test-setup using an Agilent VNA (in the back) and OML WR-03 frequency extenders (in the front).

In general TMIC fabrication is very precise, keeping circuit dimension tolerances in the submicron scale, thereto they can be designed with self-aligning features (circuit contours matched to the circuit cavities) allowing for a mounting accuracy of better than 5 μm. Waveguide blocks can be machined with better than 2 μm precision and the repeatability of waveguide interconnects can be improved by the use of waveguide standards developed for the submillimetre wave range. It is also possible to apply a statistical measurement approach by repeated measurements of a known standard or device under test. Such an approach could also be used to compensate for drift effects in the system.

A more detailed outline of the method and initial results is presented in paper [E], in [108] results on various passive components and circuits can be found. In Fig. 5.2 the waveguide block with circuit are shown together with the measured S-parameters of the thru standard after reconnection of the waveguide interfaces. In Fig. 5.3 the WR-03 test setup is shown.

Chapter 6

Summary of appended papers

In this chapter a summary of the appended papers together with comments on the creative contribution from my side is given.

Paper A

A Low VSWR 2SB Schottky Receiver

This paper discusses dual sideband topologies employing subharmonic Schottky diode mixers. A novel balanced waveguide integrated 2SB receiver based on LO and RF quadrature feeding of two subharmonic DSB mixers is demonstrated for the first time. The paper is a joint work between Omnisys Instruments AB and Chalmers University of Technology. I personally contributed with: the idea for the novel 2SB topology, design of the DSB mixers and hybrids, mechanical layout, assembly and measurements.

Paper B

Integration of a 340 GHz Subharmonic Schottky Diode Mixer and a LNA for Broadband and Low Noise Performance

In this paper the advantage of embedding the IF LNA in the mixer housing is demonstrated. The paper is a joint work between Omnisys Instruments AB, Low Noise Factory and Chalmers University of Technology. I personally contributed with: design of the DSB mixer, receiver layout, mixer assembly, measurements and simulations.

Paper C

A 170 GHz 45° Hybrid for Submillimeter Wave Sideband Separating Subharmonic Mixers

In this paper a novel 2SsB topology for submillimetre wave receivers employing subharmonic mixers is proposed. A possible realization of the LO hybrid based on a branch guide coupler with a stub-loaded differential line phase shifter at the output is demonstrated. This work was done as a collaboration between Omnisys Instruments AB and Chalmers University of Technology. I personally contributed with: the design of the hybrid, mechanical layout, measurements and simulations.

Paper D

High/Low-Impedance Transmission-Line and Coupled-Line Filter Networks for Differential Phase Shifters

In this paper two novel planar 45 degree hybrids are presented. This work was done as a collaboration between Omnisys Instruments AB and Chalmers University of Technology. I personally contributed with: the idea for the novel phase shifter topologies, theoretical analysis, design, circuit layouts, assembly and measurements.

Paper E

Submillimeter Wave S-Parameter Characterization of Integrated Membrane Circuits

In this paper a novel method for S-parameter characterization of membrane waveguide integrated circuits based on the TRL-calibration technique is proposed and demonstrated. The paper is a joint effort between SP Technical Research Institute of Sweden, Wasa Millimeter Wave AB, Omnisys Instruments AB and Chalmers University of Technology. I personally contributed with: the idea of applying this method to membrane circuits, design of TRL-kit and test circuits, circuit and mechanical layouts, assembly, measurements and simulations.

Paper F

Compact 340 GHz Receiver Front-Ends

In this paper different concepts of realising compact and cost efficient receiver front-ends including the last stage LO multipler module are discussed and partly evaluated. The low VSWR 2SB receiver topology is also proposed and a first experimental comparison between different 2SB topologies is made. The work was done as a joint effort between Wasa Millimeter Wave AB, Omnisys Instruments AB and Chalmers University of Technology. I personally contributed with: mixer design, mixer layout, mixer assembly and receiver characterisation.

Paper G

STEAMR Receiver Chain

In this paper the realisation of the STEAMR radiometer is discussed. A broadband IF spectrometer back-end based on IQ-correlator is demonstrated. The paper is a result of a Omnisys Instruments AB prestudy on the radiometer system for the STEAMR instrument, and has been done in collaboration with Chalmers University of Technology and the Swedish Space Corporation SSC. My contribution was mainly in the design and evaluation of the receiver front-end.

Paper H

Water Vapor Radiometer for ALMA

In this paper the development and evaluation of the ALMA water vapor radiometer WVR is presented in short. Omnisys Intruments AB has been responsible for the design, fabrication, assembly and final tests of the WVR's. The development of the system took 18 months and the production of the 58 radiometers took another 18 months. Final delivery to ESO was done in April 2011. My contribution was mainly in the design and evaluation of the active X6 LO multiplier and design of filter components for the IF back-end.

Chapter 7

Conclusions and future outlook

In this thesis, high functionality submillimetre wave Schottky diode mixers have been studied and practical mixer architectures including IQ-mixers and mixers with embedded LNA have been developed for the STEAMR instrument. The work has involved various aspects of mixer design i.e. mechanical design, electrical modeling, circuit design, assembly and processing as well as device and circuit characterisation. A simple and clear design methodology has also been developed for subharmonic mixers employing antiparallel diodes. The availability of commercial Schottky devices, an in-house circuit process as well as in-house manufacturing of the high precision mechanics has played a key role for this development.

The main scientific contribution of this work, has been the development of novel and practical sideband separation concepts employing subharmonic Schottky diode mixers with embedded LNA's, papers [A] and [B]. The demonstration of two novel sideband separation receivers using waveguide packaged subharmonic mixers, has been important, as efficient 2SB operation can now for the first time be considered for atmospheric sensing instruments as well as for submillimetre wave instrumentation in general.

As a side result two novel differential phase shifter topologies have been proposed and demonstrated paper [D]. The phase shifters are simple and have a minimum lateral extension.

In paper [E] a novel approach of applying TRL-calibration at submillimetre wave frequencies has been proposed and demonstrated which makes accurate characterisation of packaged THz-devices and circuits possible. The proposed method is currently being evaluated but also applied in the development of the Schottky TMIC process at Chalmers University of Technology. It will allow for the characterization of diodes as well as 2-port characterization of 3 and 4 terminal devices such as Wilkinson dividers, directional and hybrid couplers etc. needed for advanced integrated circuit topologies.

In general the prospects of developing advanced Schottky diode receivers for atmospheric observations and planetary missions seem very promising. As transistor technology is expected to become competitive to at least 300 GHz the focus for Schottky development will be at submillimetre wavelengths from 300 GHz and up, improving efficiency and functionality of receiver systems. We will see a continuous trend of integrating multiple receiver functions into single waveguide modules and on chip integration using TMIC technology for the realisation of compact, low weight, state of the art heterodyne receivers and systems. This will enable new instrument configurations and measurement methods important for atmospheric science and the understanding of climate changes. Another consequence will be that other emerging applications in the fields of security, medicine and communication will have greater probability to evolve.

Acknowledgements

First of all I would like to thank my two mentors, coaches and supervisors Jan Stake and Anders Emrich, for your perseverance and support, for believing in me and giving me the opportunity to be part of this voyage. As always a project such as this is the result of an inspirational environment created by the very people working in it. This is where seeds for new ideas and innovations are born and this is were you find the expertise and help when needed. With those words said, I would like to thank all my colleagues and friends at the Department of Microtechnology and Nanoscience, at Omnisys Instruments AB and at the Department of Radio and Space Science for all the help and support, fruitful discussions and all the good moments.

I would also like to thank my former work colleagues at Anaren Microwave Inc. and Saab Ericsson Space AB, who taught me many useful things in the art of microwave engineering.

I would like to acknowledge VDI for supplying discrete diodes and helpful discussions.

I would also like to acknowledge the financing institutions and collaboration partners. This work has been supported in part by the Swedish Research Council (VR) under grant no. 2005-2855 and at a later stage also been carried out in the GigaHertz Centre in a joint project in part financed by the Swedish Governmental Agency of Innovation Systems (VINNOVA), Chalmers University of Technology, Wasa Millimeter Wave AB, Omnisys Instruments AB and SP Technical Research Institute of Sweden.

Finally, I would like to thank my wife and family, for your love and support. Without you this would not have been possible.

Bibliography

[1] P. Siegel, "Terahertz technology," *IEEE Transactions on Microwave Theory and Techniques*, vol. 50, no. 3, pp. 910 –928, mar 2002.

[2] I. Mehdi, S. Marazita, D. Humphrey, T.-H. Lee, R. Dengler, J. Oswald, A. Pease, S. Martin, W. Bishop, T. Crowe, and P. Siegel, "Improved 240-GHz subharmonically pumped planar Schottky diode mixers for space-borne applications," *IEEE Transactions on Microwave Theory and Techniques*, vol. 46, no. 12, pp. 2036–2042, Dec. 1998.

[3] T. Crowe, W. Bishop, D. Porterfield, J. Hesler, and I. Weikle, R.M., "Opening the terahertz window with integrated diode circuits," *IEEE Journal of Solid-State Circuits*, vol. 40, no. 10, pp. 2104–2110, Oct. 2005.

[4] S. Marazita, W. Bishop, J. Hesler, K. Hui, W. Bowen, and T. Crowe, "Integrated GaAs Schottky mixers by spin-on-dielectric wafer bonding ," *IEEE Transactions on Electron Devices*, vol. 47, no. 6, pp. 1152–1157, Jun. 2000.

[5] T. Crowe, R. Mattauch, H. Roser, W. Bishop, W. Peatman, and X. Liu, "GaAs Schottky diodes for THz mixing applications," *Proceedings of the IEEE*, vol. 80, no. 11, pp. 1827–1841, Nov. 1992.

[6] European Space Agency, ESA SP-1313/5 Candidate Earth Explorer Core Missions Reports for Assessment: PREMIER Process Exploration through Measurements of Infrared and millimetre-wave Emitted Radiation, 2008, ISBN 978-92-9221-406-7, ISSN 0379-6566 .

[7] P. Siegel, "THz instruments for Space," *IEEE Transactions on Antennas and Propagation*, vol. 55, no. 11, pp. 2957–2965, Nov. 2007.

[8] T. Phillips and J. Keene, "Submillimeter astronomy [heterodyne spectroscopy]," *Proceedings of the IEEE*, vol. 80, no. 11, pp. 1662–1678, Nov. 1992.

[9] A. Wootten and A. Thompson, "The Atacama Large Millimeter/Submillimeter Array," *Proceedings of the IEEE*, vol. 97, no. 8, pp. 1463–1471, Aug. 2009.

[10] J. Kumagal, "Space mountain [submillimeter radio telescopes]," *IEEE Spectrum*, vol. 42, no. 12, pp. 12–14, Dec. 2005.

[11] D. Doyle, G. Pilbratt, and J. Tauber, "The Herschel and Planck Space Telescopes," *Proceedings of the IEEE*, vol. 97, no. 8, pp. 1403 –1411, Aug. 2009.

[12] P. Richards, "Cosmic Microwave Background experiments - past, present and future," in *Joint 32nd International Conference on Infrared and Millimeter Waves and the 15th International Conference on Terahertz Electronics, IRMMW-THz.*, Sept. 2007, pp. 12–15.

[13] Jet Propulsion Laboratory, California Institute of Technology, http://spec.jpl.nasa.gov/ .

[14] P. Siegel, "Terahertz technology in biology and medicine," in *2004 IEEE MTT-S International Microwave Symposium Digest*, vol. 3, Jun. 2004, pp. 1575 – 1578 Vol.3.

[15] E. Pickwell-MacPherson and V. Wallace, "Biomedical applications of terahertz technology," in *Journal of Physics D: Applied Physics*, vol. 39, no. 17, 2006, pp. R301 – R310.

[16] R. Appleby and H. Wallace, "Standoff detection of weapons and contraband in the 100 ghz to 1 thz region," *IEEE Transactions on Antennas and Propagation*, vol. 55, no. 11, pp. 2944 –2956, Nov. 2007.

[17] D. Glaab, S. Boppel, A. Lisauskas, U. Pfeiffer, E. Ojefors, and H. G. Roskos, "Terahertz heterodyne detection with silicon field-effect transistors," *Applied Physics Letters*, vol. 96, no. 4, pp. 042 106–042 106–3, Jan. 2010.

[18] A. Karpov, D. Miller, A. Stern, B. Bumble, H. LeDuc, and J. Zmuidzinas, "Development of 1 thz sis mixer for sofia," in *in Proc. 7th Int. Space Terahertz Technol. Symp., Pasadena, CA*, 2007, pp. 50 –53.

[19] S. Cherednichenko, V. Drakinskiy, T. Berg, P. Khosropanah, and E. Kollberg, "Hot-electron bolometer terahertz mixers for the Herschel Space Observatory," *Review of Scientific Instruments*, vol. 79, no. 3, pp. 034 501–034 501–10, Mar. 2008.

[20] W. Deal, X. Mei, V. Radisic, B. Bayuk, A. Fung, W. Yoshida, P. Liu, J. Uyeda, L. Samoska, T. Gaier, and R. Lai, "A New Sub-Millimeter Wave Power Amplifier Topology Using Large Transistors," *IEEE Microwave and Wireless Components Letters*, vol. 18, no. 8, pp. 542–544, Aug. 2008.

[21] J. Ward, G. Chattopadhyay, J. Gill, H. Javadi, C. Lee, R. Lin, A. Maestrini, F. Maiwald, I. Mehdi, E. Schlecht, and P. Siegel, "Tunable broadband frequency-multiplied terahertz sources," in *33rd International Conference on Infrared, Millimeter and Terahertz Waves, IRMMW-THz*, Sept. 2008, pp. 1–3.

[22] H.-W. Hubers, "Terahertz Heterodyne Receivers," *IEEE Journal of Selected Topics in Quantum Electronics*, vol. 14, no. 2, pp. 378–391, Mar.-Apr. 2008.

[23] O. Koistinen, H. Valmu, A. Raisanen, J. Talvela, and M. Halikainen, "A Radiometer for Ground-Based Detection of Stratospheric Ozone at 110 GHz," in *22nd European Microwave Conference*, vol. 2, Sept. 1992, pp. 1231–1233.

[24] B. Thomas, P. G. Huggard, B. Alderman, B. P. Moyna, M. L. Oldfield, B. N. Ellison, and D. N. Matheson, "Integrated Heterodyne Receivers for MM SubMM Atmospheric Remote Sensing," in *The Institution of Engineering and Technology Seminar on MM-Wave Products and Technologies*, Nov. 2006, pp. 13–18.

[25] C. Groppi, R. Kursinski, D. Ward, A. Otarola, K. Sammler, M. Schein, S. Al Banna, B. Wheelwright, S. Bell, W. Bertiger, M. Miller, and H. Pickett, "ATOMMS: the Active Temperature, Ozone and Moisture Microwave Spectrometer," in *Twentieth International Symposium on Space Terahertz Technology, Charlottesville*, Apr. 2009, pp. 167–173.

[26] I. Yoshihisa, T. Manabe, S. Ochiai, H. Masuko, T. Yamagami, Y. Saito, N. Izutsu, T. Kawasaki, M. Namiki, K. Sato, and I. Murata, "A balloon-borne 620-650 GHz SIS receiver for atmospheric observations," in *IEEE International Geoscience and Remote Sensing Symposium, IGARSS*, vol. 1, Jul. 2005, p. 4.

[27] Japan Aerospace Exploration Agency, JAXA, http://www.isas.jaxa.jp/e/enterp/rockets/sounding/index.shtml
.

[28] "Global observations of middle atmospheric water vapour by the odin satellite: An overview," *Planetary and Space Science*, vol. 55, no. 9, pp. 1093–1102, 2007, highlights in Planetary Science, 2nd General Assembly of Asia Oceania Geophysical Society.

[29] J. W. et. al., "The Earth Observing System Microwave Limb Sounder(EOS MLS) on the Aura Satellite," *IEEE Transactions on Geoscience and Remote Sensing*, vol. 44, no. 5, pp. 1075–1092, May. 2006.

[30] N. Skou and D. L. Vine, *Microwave Radiometer Systems: Design and Analysis, Second Edition* . Artech House, 2006.

[31] M. Griffin, G. Pilbratt, T. de Graauw, and A. Poglitsch, "The Herschel Space Observatory," in *33rd International Conference on Infrared, Millimeter and Terahertz Waves, IRMMW-THz*, Sept. 2008, pp. 1–2.

[32] H. Sugita, T. Nakagawa, H. Murakami, A. Okamoto, H. Nagai, M. Murakami, K. Narasaki, and M. Hirabayashi, "Cryogenic infrared mission "JAXA/SPICA" with advanced cryocoolers," *Cryogenics"*, vol. 46, no. 2-3, pp. 149–157, 2006, 2005 Space Cryogenics Workshop.

[33] P. Lehikoinen, J. Mallat, P. Piironen, A. Lehto, J. Tuovinene, and A. V. Räisänen, "A 119 GHz planar Schottky diode mixer for a space application," *International Journal of Infrared and Millimeter Waves*, vol. 17, pp. 807–818, May 1996.

[34] P. Siegel, R. Dengler, I. Mehdi, W. Bishop, and T. Crowe, "A 200 GHz planar diode subharmonically pumped waveguide mixer with state-of-the-art performance," in *IEEE MTT-S International Microwave Symposium Digest*, Jun. 1992, pp. 595–598, Vol.2.

[35] W. Y. Ali-Ahmad, W. L. Bishop, T. W. Crowe, and G. M. Rebeiz, “A 250 GHz planar low noise Schottky receiver,” *International Journal of Infrared and Millimeter Waves*, vol. 14, pp. 737–748, Apr. 1993.

[36] S. Rea, B. Thomas, and D. Matheson, “A 320-360 GHz Sub-Harmonically pumped Image-Rejection Mixer for earth observation applications,” Sept. 2008, p. 1.

[37] J. Hesler, K. Hui, S. He, and T. Crowe, “A Fixed-Tuned 400 GHz Subharmonic Mixer using Planar Schottky Diodes,” in *Tenth International Symposium on Space Terahertz Technology, Charlottesville*, Mar. 1999, pp. 95–99.

[38] B. Thomas, A. Maestrini, and G. Beaudin, “A low-noise fixed-tuned 300-360-GHz sub-harmonic mixer using planar Schottky diodes,” *IEEE Microwave and Wireless Components Letters*, vol. 15, no. 12, pp. 865–867, Dec. 2005.

[39] K. Hui, J. Hesler, D. Kurtz, W. Bishop, and T. Crowe, “A micromachined 585 GHz Schottky mixer,” *IEEE Microwave and Guided Wave Letters*, vol. 10, no. 9, pp. 374–376, Sept. 2000.

[40] M. Boheim, L.-P. Schmidt, J. Ritter, V. Brankovic, R. Beyer, F. Arndt, U. Klein, K. Kunzi, G. Schwaab, and T. W. Crowe, “A New 140 GHz Planar Diode Finline Mixer for Radiometer Applications,” in *24th European Microwave Conference*, vol. 1, Sept. 1994, pp. 664–669.

[41] W. Bishop, K. McKinney, R. Mattauch, T. Crowe, and G. Green, “A Novel Whiskerless Schottky Diode for Millimeter and Submillimeter Wave Application,” in *MTT-S International Microwave Symposium Digest*, vol. 87, no. 2, June 1987, pp. 607–610.

[42] S. Gearhart, J. Hesler, W. Bishop, T. Crowe, and G. Rebeiz, “A wideband 760-GHz planar integrated Schottky receiver,” *IEEE Microwave and Guided Wave Letters*, vol. 3, no. 7, pp. 205–207, July 1993.

[43] J. Hesler, “Broadband Fixed-Tuned Subharmonic Receivers to 640 GHz,” in *Eleventh International Symposium on Space Terahertz Technology*, 2000, pp. 3–5.

[44] B. Moyna, C. Mann, B. Ellison, M. Oldfield, D. Matheson, and T. Crowe, “Broadband space-qualified subharmonic mixers at 183 GHz with low local oscillator power requirements,” in *2nd ESA Workshop on MM-Wave Technology Applications: Antennas, Circuits Systems, Espoo, Finland*, May 1998, pp. 3–5.

[45] S. Vogel, “Design and measurements of a novel subharmonically pumped millimeter-wave mixer using two single planar Schottky-barrier diodes ,” *IEEE Transactions on Microwave Theory and Techniques*, vol. 44, no. 6, pp. 825–831, Jun. 1996.

[46] J. Hesler, D. Porterfield, W. Bishop, T. Crowe, and P. Racette, “Development of compact broadband receivers at submillimeter wavelengths,” in *IEEE Aerospace Conference Proceedings*, vol. 2, Mar. 2004, pp. 735–740, Vol.2.

[47] J. Hesler, W. Hall, T. Crowe, I. Weikle, R.M., J. Deaver, B.S., R. Bradley, and S.-K. Pan, "Fixed-tuned submillimeter wavelength waveguide mixers using planar Schottky-barrier diodes," *IEEE Transactions on Microwave Theory and Techniques*, vol. 45, no. 5, pp. 653–658, May 1997.

[48] I. Mehdi, S. Marazita, D. Humphrey, T.-H. Lee, R. Dengler, J. Oswald, A. Pease, S. Martin, W. Bishop, T. Crowe, and P. Siegel, "Improved 240-GHz subharmonically pumped planar Schottky diode mixers for space-borne applications," *IEEE Transactions on Microwave Theory and Techniques*, vol. 46, no. 12, pp. 2036–2042, Dec. 1998.

[49] D. Porterfield, J. Hesler, T. Crowe, W. Bishop, and D. Woolard, "Integrated terahertz transmit/receive modules," in *33rd European Microwave Conference*, vol. 3, Oct. 2003, pp. 1319–1322, Vol.3.

[50] S. Marazita, K. Hui, J. Hesler, W. Bishop, and T. Crowe, "Progress in Submillimeter Wavelength Integrated Mixer Technology," in *Tenth International Symposium on Space Terahertz Technology, Charlottesville*, Mar. 1999, pp. 95–99.

[51] Virginia Diodes Inc., www.virginiadiodes.com.

[52] N. Erickson, "A Very Low-Noise Single-Sideband Receiver for 200-260 GHz," *IEEE Transactions on Microwave Theory and Techniques*, vol. 33, no. 11, pp. 1179–1188, Nov. 1985.

[53] B. Thomas, P. G. Huggard, B. Alderman, B. P. Moyna, M. L. Oldfield, B. N. Ellison, and D. N. Matheson, "Integrated Heterodyne Receivers for MM SubMM Atmospheric Remote Sensing," in *The Institution of Engineering and Technology Seminar on MM-Wave Products and Technologies*, Nov. 2006, pp. 13–18.

[54] S. B. Rozanov, A. N. Lukin, and S. V. Solomonov, "Low-noise cooled planar Schottky diode receivers for ground-based spectral ozone measurements at 142 GHz," *International journal of infrared and millimeter waves*, vol. 19, no. 2, pp. 195–222, 1998.

[55] W. Zhang, P. Khosropanah, J. R. Gao, E. L. Kollberg, K. S. Yngvesson, T. Bansal, R. Barends, and T. M. Klapwijk, "Quantum noise in a terahertz hot electron bolometer mixer," *Applied Physics Letters*, vol. 96, no. 11, pp. 111 113–1–3, Mar. 2010.

[56] A. Tessmann, A. Leuther, M. Kuri, H. Massler, M. Riessle, H. Essen, S. Stanko, R. Sommer, M. Zink, R. Stibal, W. Reinert, and M. Schlechtweg, "220 GHz Low-Noise Amplifier Modules for Radiometric Imaging Applications," in *The 1st European Microwave Integrated Circuits Conference*, Sept. 2006, pp. 137–140.

[57] H. Wang, R. Lai, Y.-L. Kok, T.-W. Huang, M. Aust, Y. Chen, P. Siegel, T. Gaier, R. Dengler, and B. Allen, "A 155-GHz monolithic low-noise amplifier," *IEEE Transactions on Microwave Theory and Techniques*, vol. 46, no. 11, pp. 1660–1666, Nov. 1998.

[58] R. Lai, W. Deal, V. Radisic, K. Leong, X. Mei, S. Sarkozy, T. Gaier, L. Samoska, and A. Fung, "Sub-MMW active integrated circuits based on 35 nm InP HEMT technology," in *IEEE International Conference on Indium Phosphide Related Materials, IPRM*, May 2009, pp. 185–187.

[59] P. Kangaslahti, D. Pukala, T. Gaier, W. Deal, X. Mei, and R. Lai, "Low noise amplifier for 180 GHz frequency band," in *IEEE MTT-S International Microwave Symposium Digest*, June 2008, pp. 451–454.

[60] S. Gunnarsson, N. Wadefalk, J. Svedin, S. Cherednichenko, I. Angelov, H. Zirath, I. Kallfass, and A. Leuther, "A 220 GHz Single-Chip Receiver MMIC With Integrated Antenna," *IEEE Microwave and Wireless Components Letters*, vol. 18, no. 4, pp. 284–286, Apr. 2008.

[61] H. Zirath, N. Wadefalk, R. Kuzhuharov, S. Gunnarson, S. Cherednichenko, I. Angelov, M. Abbasi, B. Hansson, V. Vassilev, J. Svedin, S. Rudner, I. Kallfass, and A. Leuther, "Integrated receivers up to 220 GHz utilizing GaAs-mHEMT technology ," in *IEEE German Microwave Conference, GeMMIC*, Dec. 2010, pp. 225 –228.

[62] M. Cohn, J. Degenford, and B. Newman, "Harmonic Mixing with an Anti-Parallel Diode Pair," in *MTT International Microwave Symposium Digest*, vol. 74, no. 1, Jun. 1974, pp. 171–172.

[63] I.-H. Lin, K. Leong, C. Caloz, and T. Itoh, "Dual-band subharmonic quadrature mixer using composite right/left-handed transmission lines," *IEE Proceedings - Microwaves, Antennas and Propagation*, vol. 153, no. 4, pp. 365–375, Aug. 2006.

[64] T. Yamaji, H. Tanimoto, and H. Kokatsu, "An I/Q active balanced harmonic mixer with IM2 cancelers and a 45 deg; phase shifter," in *IEEE International Solid-State Circuits Conference, Digest of Technical Papers*, vol. 33, no. 12, Dec. 1998, pp. 2240 –2246.

[65] V. Vassilev, D. Henke, I. Lapkin, O. Nyström, R. Monje, A. Pavolotsky, and V. Belitsky, "Design and Characterization of a 211 GHz Sideband Separating Mixer for the APEX Telescope," *IEEE Microwave and Wireless Components Letters*, vol. 18, no. 1, pp. 58–60, Jan. 2008.

[66] B. Thomas, S. Rea, B. Moyna, B. Alderman, and D. Matheson, "A 320-360 GHz Subharmonically Pumped Image Rejection Mixer Using Planar Schottky Diodes," *IEEE Microwave and Wireless Components Letters*, vol. 19, no. 2, pp. 101–103, Feb. 2009.

[67] D. Allan, "Statistics of atomic frequency standards," *Proceedings of the IEEE*, vol. 54, no. 2, pp. 221 –230, Feb. 1966.

[68] T. Berg, S. Cherednichenko, V. Drakinskiy, H. Merkel, E. Kollberg, and J. W. Kooi, "Stability measurements of an NbN HEB receiver at THz frequencies ," in *Fifteenth International Symposium on Space Terahertz Technology, Northampton, Massachusetts, USA*, Apr. 2004, pp. 25–32.

[69] Modelling and characterization of a broadband 85 to 170 GHz Schottky varactor frequency doubler, Thesis for the degree of Master of Science in Integrated Electronic System Design,Chalmers University of Technology, $G\ddot{o}teborg, Sweden.$

[70] A. R. Kerr, M. J. Feldman, and S.-K. Pan, "Receiver Noise Temperature, the Quantum Noise Limit, and the Role of the Zero-Point Fluctuations," in *8th Int. Symp. on Space Terahertz Tech.*, Mar. 1997, pp. 101–111.

[71] P. Marsh, D. Pavlidis, and K. Hong, "Ingaas-schottky contacts made by in situ plated and evaporated pt-an analysis based on dc and noise characteristics," *IEEE Transactions on Electron Devices*, vol. 45, no. 2, pp. 349 –360, Feb. 1998.

[72] "Inteface-controlled schottky barriers on inp and related materials," *Solid-State Electronics*, vol. 41, no. 10, pp. 1441 – 1450, 1997, proceedings of the Topical Workshop on Heterostructure of Microlectronics.

[73] A. Kerr, "Noise and loss in balanced and subharmonically pumped mixers: Part i–theory," *IEEE Transactions on Microwave Theory and Techniques*, vol. 27, no. 12, pp. 938 – 943, Dec. 1979.

[74] ——, "Noise and loss in balanced and subharmonically pumped mixers: Part ii–application," *IEEE Transactions on Microwave Theory and Techniques*, vol. 27, no. 12, pp. 944 – 950, Dec. 1979.

[75] E. Kollberg and A. Rydberg, "Quantum-barrier-varactor diodes for high-efficiency millimetre-wave multipliers," *Electronics Letters*, vol. 25, no. 25, pp. 1696–1698, Dec. 1989.

[76] H. Friis, "A Note on a Simple Transmission Formula," *Proc. IRE*, pp. 254–256, May. 1946.

[77] K. Yhland, "Simplified Analysis of Resistive Mixers," *IEEE Microwave and Wireless Components Letters*, vol. 17, no. 8, pp. 604–606, Aug. 2007.

[78] W. Kelly and G. Wrixon, "Conversion Losses in Schottky-Barrier Diode Mixers in the Submillimeter Region," *IEEE Transactions on Microwave Theory and Techniques*, vol. 27, no. 7, pp. 665–672, Jul. 1979.

[79] M. McColl, "Conversion Loss Limitations on Schottky-Barrier Mixers (Short Papers)," *IEEE Transactions on Microwave Theory and Techniques*, vol. 25, no. 1, pp. 54–59, Jan. 1977.

[80] W. Schottky, *Phys. Z.*, vol. 41, p. 570, 1940.

[81] F. Braun, "Uber die stromleitung durch schwefelmetalle," *Annalen der Physik*, vol. 229, no. 12, pp. 556–563, 1875.

[82] A. Cowley and S. Sze, "Surface States and Barrier Height of Metal-Semiconductor Systems," *Journal of Applied Physics*, vol. 36, no. 10, p. 3212, 1965.

[83] S. Sze, C. Crowell, and D. Kahng, "Photoelectric Determination of Image Force Dielectric Constant For Hot Electrons in Schottky Barriers," *Journal of Applied Physics*, vol. 35, no. 8, p. 2534, 1964.

[84] J. Bardeen, "Surface States and Rectification at a Metal Semi-Conductor Contact," *Physical Review*, vol. 71, no. 10, pp. 717–727, 1947.

[85] R. Fano, “Theoretical limitations on the broadband matching of arbitrary impedances,” *J. Franklin Inst.*, vol. 249, pp. 57 –83, Jan. 1950.

[86] L. Dickens, “Spreading resistance as a function of frequency,” *IEEE Transactions on Microwave Theory and Techniques*, vol. 15, no. 2, pp. 101 –109, Feb. 1967.

[87] J. L. Hesler, “Planar Schottky Diodes in Submillimeter-Wavelength Waveguide Receivers,” Ph.D. dissertation, School of Engineering and Applied Science, University of Virginia, Charlottesville, United States, 1996.

[88] H. A. Wheeler, “Formulas for the skin effect,” *Proceedings of the IRE*, vol. 30, no. 9, pp. 412–424, 1942.

[89] H. Xu, G. Schoenthal, L. Liu, Q. Xiao, J. Hesler, and R. Weikle, “On Estimating and Canceling Parasitic Capacitance in Submillimeter-Wave Planar Schottky Diodes,” *IEEE Microwave and Wireless Components Letters*, vol. 19, no. 12, pp. 807–809, Dec. 2009.

[90] A.-Y. Tang and J. Stake, “Impact of eddy currents and crowding effects on high frequency losses in planar schottky diodes,” *submitted to Transactions on Electron Devices*, Mar. 2011.

[91] S. A. Maas, *Noise in linear and nonlinear circuits, Artech House, 2005.*

[92] H. Nyquist, “Thermal agitation of electric charge in conductors,” *Physical Review*, vol. 32, no. 1, pp. 110–113, 1928.

[93] J. Johnson, “Thermal agitation of electricity in conductors,” *Physical Review*, vol. 32, no. 1, pp. 97–109, 1928.

[94] T. W. Crowe, “Modeling and optimization of GaAs Schottky barrier mixer diodes,” Ph.D. dissertation, School of Engineering and Applied Science, University of Virginia, Charlottesville, United States, 1986.

[95] T. Crowe and R. Mattauch, “Analysis and optimization of millimeter- and submillimeter-wavelength mixer diodes,” *IEEE Transactions on Microwave Theory and Techniques*, vol. 35, no. 2, pp. 159 – 168, Feb. 1987.

[96] E. Schlecht, J. Gill, R. Dengler, R. Lin, R. Tsang, and I. Mehdi, “A Unique 520-590 GHz Biased Subharmonically-Pumped Schottky Mixer,” *IEEE Microwave and Wireless Components Letters*, vol. 17, no. 12, pp. 879–881, Dec. 2007.

[97] R. Eisenhart and P. Khan, “Theoretical and experimental analysis of a waveguide mounting structure,” *IEEE Transactions on Microwave Theory and Techniques*, vol. 19, no. 8, pp. 706 – 719, aug 1971.

[98] V. Vassilev, V. Belitsky, D. Urbain, and S. Kovtonyuk, “A new 3-dB power divider for millimeter-wavelengths,” *IEEE Microwave and Wireless Components Letters*, vol. 11, no. 1, pp. 30–32, Jan. 2001.

[99] T.-H. Lin and R.-B. Wu, “A Broadband Microstrip-to-Waveguide Transition with Tapered CPS Probe,” in *32nd European Microwave Conference*, Sept. 2002, pp. 1–4.

[100] Z. Tong, A. Stelzer, W. Menzel, C. Wagner, R. Feger, and E. Kolmhofer, “A wide band transition from waveguide to differential microstrip lines,” in *Asia-Pacific Microwave Conference, APMC*, 2009.

[101] W. R. Deal, X. B. Mei, V. Radisic, K. Leong, S. Sarkozy, B. Gorospe, J. Lee, P. H. Liu, W. Yoshida, J. Zhou, M. Lange, J. Uyeda, and R. Lai, “Demonstration of a 0.48 THz Amplifier Module Using InP HEMT Transistors,” *IEEE Microwave and Wireless Components Letters*, vol. 20, no. 5, pp. 289 –291, May 2010.

[102] G. Ponchak and R. Simons, “A new rectangular waveguide to coplanar waveguide transition,” in *IEEE MTT-S International Microwave Symposium Digest*, May 1990, pp. 491–492, Vol.1.

[103] A. Kerr and J. Randa, “Thermal Noise and Noise Measurements A 2010 Update,” *IEEE Microwave Magazine*, vol. 11, no. 6, pp. 40–52, Oct. 2010.

[104] A. Fung, D. Dawson, L. Samoska, K. Lee, T. Gaier, P. Kangaslahti, C. Oleson, A. Denning, Y. Lau, and G. Boll, “Two-port vector network analyzer measurements in the 218-344 ghz and 356-500 ghz frequency bands,” *IEEE Transactions on Microwave Theory and Techniques*, vol. 54, no. 12, pp. 4507 –4512, Dec. 2006.

[105] Virginia Diodes Inc., http://www.virginiadiodes.com .

[106] T. Reck, L. Chen, C. Zhang, C. Groppi, H. Xu, A. Arsenovic, N. Barker, A. Lichtenberger, and R. Weikle, “Micromachined on-wafer probes,” in *2010 IEEE MTT-S International Microwave Symposium Digest (MTT)*, May 2010, pp. 65 –68.

[107] A. R. Kerr and S. Srikanth, “The ring-centred waveguide flange for submillimetre wavelength,” in *Twentieth International Symposium on Space Terahertz Technology, Charlottesville*, Apr. 2009, pp. 220–222.

[108] H. Zhao, T. Ngoc Thi Do, P. Sobis, A.-Y. Tang, K. Yhland, J. Stenarsson, and J. Stake, “Characterization of thin film resistors and capacitors integrated on GaAs membranes for submillimeter wave circuit applications,” in *23rd International Conference on Indium Phosphide and Related Materials IPRM, Berlin, Germany*, May 2011.

Paper A

A Low VSWR 2SB Schottky Receiver

P. Sobis, J. Stake, and A. Emrich

submitted to *IEEE Terahertz Science and Technology*, Apr. 2011.

Paper B

Integration of a 340 GHz Subharmonic Schottky Diode Mixer and a LNA for Broadband and Low Noise Performance

P. Sobis, N. Wadefalk, A. Emrich, and J. Stake

submitted to *IEEE Terahertz Science and Technology*, Apr. 2011.

Paper C

A 170 GHz 45° Hybrid for Submillimeter Wave Sideband Separating Subharmonic Mixers

P. Sobis, J. Stake, and A. Emrich

in *IEEE Microwave and Wireless Components Letters*, vol. 18, no. 10, pp. 680–682, Oct. 2008.

Paper D

High/Low Impedance Transmission Line and Coupled Line Filter Networks for Differential Phase Shifters

P. Sobis, J. Stake, and A. Emrich

in *IEEE Microwaves, Antennas and Propagation*, vol. 5, no. 4, pp. 386–392, Mar. 2011.

Paper E

Submillimeter Wave S-Parameter Characterization of Integrated Membrane Circuits

H. Zhao, A-Y. Tang, P. Sobis, T. Bryllert, J. Stake, K. Yhland and J. Stenarson

in *IEEE Microwave and Wireless Components Letters*, vol. 21, no. 2, pp. 110–112, Feb. 2011.

Paper F

Compact 340 GHz Receiver Front-Ends

P. Sobis, T. Bryllert, A. Olsen, J. Vukusic, V. Drakinskiy, S. Cherednichenko, A. Emrich, and J. Stake

in *20th International Symposium on Space Terahertz Technology (ISSTT), Charlottesville, VA, USA*, pp. 183–189, Apr. 2009.

Paper G

STEAMR Receiver Chain

P. Sobis, A. Emrich, and M. Hjorth

in *20th International Symposium on Space Terahertz Technology (ISSTT), Charlottesville, VA, USA*, pp. 320–325, Apr. 2009.

Paper H

Water Vapor Radiometer for ALMA

A. Emrich, S. Andersson, M. Wannerbratt, P. Sobis, S. Cherednichenko, D. Runesson, T. Ekebrand, M. Krus, C. Tegnander and U. Krus

in *20th International Symposium on Space Terahertz Technology (ISSTT), Charlottesville, VA, USA*, pp. 174–177, Apr. 2009.